TRW Technical Report No.: 46179-6041-UT-00

FINAL REPORT

ISEE/ICE Plasma Wave Data Analysis

Contract NO. NAS5-26903

Principal Investigator: E. W. Greenstadt

Report for Period:

January 1985-October 1989

Prepared for:

NASA Goddard Space Flight Center
Greenbelt, Maryland

October 1989

TRW Space and Technology Group
Applied Technology Division
Bldg. R1, Room 1176
One Space Park
Redondo Beach, California 90278

TABLE OF CONTENTS

PREFACE

The purpose of this report is to summarizthe performance of work for the period 1 January 1985 through 30 October 1989, in compliance with Modification 13 of Contract NAS5-28703. The objective of this contract has been to provide reduction and analysis of data from a scientific instrument designed to study solar wind and plasma wave phenomena on the ISEE-3/ICE missions.

INTRODUCTION

This is a final report covering the ICE/ISEE-3 Plasma Wave (PW) Investigation for the period January 1985 through October 1989. This report therefore closes the latest contract period, following previous quarterly reports and a chain of semiannual reports from preceding contracts. The instrument was described in a paper by F. L. Scarf, R. W. Fredricks, D. A. Gurnett, and E. J. Smith: "The ISEE-C Plasma Wave Instrument," in IEEE Trans. Geosci. Elect., GE-16, pp191-195, 1978. Processing, research, and publication have been sustained by GSFC contracts NAS5-20682 and NAS5-28703 (TRW Sales Numbers 23499 and 46179, respectively), under which quarterly and semiannual reports were submitted regularly describing the research results obtained and listing the associated, reviewed publications.

Since launch of ISEE-3, or ISEE-C, in 1978, its PW team and collaborators have published or prepared over 50 written reports, some currently pending, describing results on the solar wind, solar activity, interplanetary shocks, and planetary and cometary interaction regions. Data have been shared with other investigators and nine years of microfiche plots of the data have been deposited with NSSDC.

At the beginning of this Contract period, ICE was on its way to comet Giacobini-Zinner (G-Z), where it arrived in September 1985 to become the first spacecraft to explore the environment of a comet. This phase of the mission was a monumental success, despite some decimation of ICE's instrument complement. We are pleased to record that the Plasma Wave (PW) Detector was one of the instruments still operating well and that it made vital contributions to mankind's first direct record of an instrumented encounter with cometary plasma.

Unhappily, this enormously successful period of ISEE-3/ICE operation was disfigured by the sudden, tragic death of Dr. Frederick L. Scarf, the Plasma Wave Detector's Principal Investigator (PI) and also the main scientific driver behind the actions that recreated ISEE-3 as a new mission and sent it on its way to G-Z, as International Cometary Explorer. The sole consolation of those who worked with Fred on this project was that he lived to experience the dramatic realization of the ICE rationale and, indeed, to see the publication of many of the results from his own and other instruments.

An inevitable consequence of the dreadful event of the last paragraph was, of course, to make a change of PI one of the major occurrences of this reporting period. This report is written by the new PI, Eugene W. Greenstadt, who, thinking of scientific continuity and data processing as the highest priorities for the ICE PW program, has assigned only limited resources to recon-

structing details of the the first two years of this Contract period from Fred's extensive files, relying instead on published documents to speak for the program's activities and accomplishments. The report period is naturally divided into subintervals by Fred's death, the first defined by the record left by the original PI, the second by the experience and attention of his successor. In the ensuing sections, we synopsize our activities, divided as just described, and the principal scientific results, list our presentations and publications, and conclude with a brief SUMMARY AND CRITIQUE. Miscellaneous documentation of scientific results are provided in Appendices, as explained in the body of the report.

ACTIVITIES

January 1985 to July 1988

Scientific activities under this Contract before July 1988 are best summarized by the publications of the original Principal Investigator and his colleagues. Appendix D is a list of all papers whose publication dates fell within, or whose manuscripts were prepared wholly during, this first division of the current period.

Much of the preparation of the articles published in 1985 took place, of course, in an earlier funded period; we have not tried to distinguish reports prepared only after January 1985. No attempt has been made either to reconstruct the nonresearch activities of Dr. Scarf, activities which included management, discussion, and analysis of data, and attendance at numerous meetings, panels, and conferences, where his contributions were undoubtedly invaluable to the ICE/ISEE-3 project.

Routine processing of ICE plasma wave data, an activity whose latest status only is of interest, is covered as a cumulative result in a later section, regardless of whether it took place before or after July 1988.

July 1988 to present

Fred Scarf's death almost coincided with the decline of a surge of reports following the period of concentration on ICE's G-Z encounter. Although interest in the G-Z data continues at a reduced level, attention has shifted toward two other aspects of the ISEE-3/ICE missions: The prolific sampling by ISEE-3 in 1982-83 of Earth's distant downwind foreshock, bow shock, magnetosheath, and magnetotail; and the interplanetary cruise of ICE that began after it left the G-Z environment. Both of these components of the ISEE-3/ICE program are relatively unexploited and at the beginning of their productive cycles. Also, the main interest in the interplanetary cruise of ICE has centered so far on increasing solar activity and the coronal mass ejections

(CME's) that are sure to accompany it, but CME's are unpredictable chance events, not programmed "targets". Hence, few immediate research results can be expected. Preliminary assessment of these components is in progress.

For the PW experiment specifically, Fred's death precipitated a period of distraction, reorganization, reassessment, and retrenchment some of which lingers to this hour, and which constituted much of the activity of the second half of 1988 and the beginning of 1989. Our scientific effort had recovered momentum by early 1989, however, as we continued studies already underway and initiated some new approaches to our data handling and scientific objectives.

Organization. An acting Project Manager, Eugene W. Greenstadt, was quickly appointed by TRW in Fred's place, and later Mr. Greenstadt was named by NASA as new Principal Investigator for the ICE Plasma Wave Detector. The administrative status of the project was reviewed, pending deadlines for proposals to continue the program in 1989 were written, submitted, and approved and funded by NASA/GSFC. Current and future scientific objectives also were reviewed in consultation with colleagues associated with the ICE Plasma Wave project. New goals were determined and a new approach to data processing was launched.

Processing and Archiving. At the time of writing, ICE Plasma Wave data have been processed to produce our standard multichannel plots covering acquired data through 31 July 1989. All plots from January 1987 through December 1988 have been sorted and are ready to be copied as microfiche. We expect these to be completed and sent to NSSDC for archiving by the end of this Contract.

We have been developing, in cooperation with Dr Robert Strangeway of UCLA, plans for producing and using Dr. Strangeway's spectrogram format of the multichannel data to compress the display of solar wind observations for studying long term patterns of plasma waves through the solar cycle. If this approach is successful, we plan to make the hoped-for synoptic views of our interplanetary data available to other investigators and NSSDC.

Analysis. We supported or conducted analysis under four topics:

1. Ion pickup at G-Z. Final figures were prepared and supplied for publication of a report in process at the time of Fred's death.

2. Tail boundaries. Detailed analysis of the occurrence and spectra of plasma waves in and around the principal boundaries of the distant magnetotail were completed.

3. Downwind interval. A survey of the traversals and encounters of ISEE-3 with the distant magnetosheath, bow shock, and fore-

shock was conducted and an appraisal made of the value of the data during the satellite's observations of these regions.

4. CME's. Preliminary data were processed and examined for an interval in 1989 named by colleagues as potentially interesting as a record of a CME events. Optimal arrangements of the plasma wave data to take better advantage of such intervals were explored.

RESEARCH RESULTS

Ion pickup at G-Z

Plasma wave data obtained in the ion pickup region surrounding comet Giacobini-Zinner were compared with energetic particle data and found consistent with theories of emissions from both pickup photoelectrons, via beam instability, and pickup ions, via ring-type instability.

Tail boundaries

Moderate to intense electric field disturbances, in the form of plasma waves, were found in various amplitudes and spectral distributions in a variety of boundaries of the magnetotail. Different spectra were associated with the magnetotail lobes and with the magnetopause and plasma sheet boundary layers. Subtle, but distinguishable changes in spectra were noted as boundaries were crossed. Some of the oscillations suggested the presence of cold dense electrons.

Downwind interval

The many, and prolonged, passages of ISEE-3 through the distant solar wind-magnetospheric interaction region were found to provide unique observations of the magnetosheath, shock, and foreshock never before available. Cases in which ISEE-3 was sampling one or another interaction phenomenon while ISEE-1,2 were upstream in the solar wind were numerous, encouraging the prospect of correlated study of the distant interaction processes. Over 100 shock crossings were detected, mostly at low Mach number, many with locally quasi-parallel geometry, constituting plasma parameter combinations rare in space plasma experience. The best model currently available for representing the global shock shape along its flank was found to agree well with the locations of the recorded shock crossings.

CME's

Motivated by reports of possible CME activity spanning late May and early June 1989, we processed a week's worth of plasma wave data to test for detectable levels of wave enhancement. The results were disappointing, primarily for two reasons: First, we

realized how unfamiliar we were with the plasma wave character of the solar wind, both disturbed and undisturbed, over typical time scales of major solar activity events; we could not expect a priori to distingish a CME from any other source of sporadic plasma wave signals in the interplanetary medium. Second, the duty cycle in effect for the interval we processed was so low and irregular that we had no possibility of using the data during, or surrounding, the prospective CME to correct our ignorance, let alone gain an insight into the profile of the event in question. We determined therefore to experiment with compressed data formats to expose long term plasma wave patterns in the solar wind which we can use in future as background to investigate CME occurrences. The formats will include spectrograms averaged in various ways to be determined by experimentation.

REPORTS

If a report of a research result has been published, it is listed in the Publications subsection below, and its Abstract is reproduced in an Appendix. If a report is yet unpublished, it is listed here and reproduced in its entirety in an Appendix.

Coroniti, F. V., E. W. Greenstadt, B. T. Tsurutani, E. J. Smith, R. D. Zwickl, and J. T. Gosling, Plasma waves in the distant geomagnetic tail, scheduled for submission to J. Geophys. Res. (unreviewed draft version in Appendix A)

Greenstadt, E. W., D. P. Traver, F. V. Coroniti, E. J. Smith, and J. A. Slavin, Observations of the flank of the earth's bow shock to -110 R_E by ISEE-3, intended for submission to Geophys. Rev. Lett. (unreviewed draft version in Appendix B)

PRESENTATIONS AND PUBLICATIONS

Presentations

The two reports listed in the previous section were given as poster papers at the Spring meeting of the American Geophysical Meeting, Baltimore, May, 1989. In addition, a review talk that included reference to ISEE-3/ICE plasma wave data was given at the same meeting:

Moses, S. L., Plasma waves at collisionless shocks in space: The observations of F. L. Scarf.

Publications

The following, posthumous publication with Fred Scarf as coauthor was completed with the assistance of the successor PI. The abstract is copied in APPENDIX C.

Richardson, I. G., K.-P Wenzel, S. W. H. Cowley, F. L. Scarf, E.

J. Smith, B. T. Tsurutani T. R. Sanderson, and R. J. Hynds, Correlated plasma wave, magnetic field, and energetic ion observations in the ion pickup region of comet Giacobini-Zinner, J. Geophys. Res., 94, 49-59, 1989.

Related Investigations

Two reports related to future ISEE-3/ICE studies, although not drawing on ISEE-3 data or funds, were prepared, presented, and/or completed this year:

Greenstadt, E. W., J. T. Gosling, M. F. Thomsen, and C. T. Russell, Thin shock transitions coincident with instantateously high O_{Bn} in quasiparallel structures, presented to IAGA, Exeter, August, 1989; draft paper almost complete for submission to J. Geophys. Res.

Kennel, C. F., F. V. Coroniti, S. L. Moses, and L. M. Zelenyi, Dynamics of Mars' magnetosphere, Geophys. Res. Lett., 16, 915-918, 1989.

SUMMARY AND CRITIQUE

The period of this Contract was one of the most productive of the ISEE-3/ICE missions, because of the intense interest in the ICE flyby of comet Giacobini-Zinner in 1985. Data from the Plasma Wave detector at G-Z were contained in 18 of the presentations and publications in APPENDIX D, and prominently in nine of them with Scarf as first author. Plasma wave signals proved themselves again to be both sensitive markers of features of every sort in space plasmas, powerful clues to the various states of disequilibrium responsible for local electric and electromagnetic instabilities, and effective testers of theoretical predictions of the effects of these instabilities. Linear and nonlinear wave-wave interactions, inter- and counter-streaming particle beams, ring distributions, flux ropes, slow shocks, and plasma boundary surfaces have all provided natural conditions or sites for significant plasma wave activity.

Although important characteristics of comet G-Z still remain to be illuminated, the untargeted post-G-Z phase of the ICE mission has opened the entire ISEE-3/ICE program to reassessment of the unexploited treasures accumulated in its data base since launch. The rising sunspot numbers of the current solar activity cycle furnish inspiration for one major topic of future research, namely, coronal mass ejections and the transient phenomena associated with them that ICE instruments may even now be recording. We are eager to explore these phenomena with the PW detector, but such exploration will require more sophisticated approaches to data processing than has been employed so far. We believe that ISEE-3's initial solar wind phase, its extensive sampling of

Earth's distant downwind magnetosheath, shock, and foreshock, ICE's cruise to G-Z, and the G-Z encounter also contain information that would benefit from renewed scrutiny, and a fresh analysis of the data with processing techniques different from those already applied, including spatial overlays and synoptic spectrograms.

APPENDIX A

Coroniti et al., DRAFT Report

APPENDIX A

Coroniti et al., DRAFT Report

Plasma Waves in the Distant Geomagnetic Tail

by

F.V. Coroniti[1], E.W. Greenstadt[1], B.T. Tsurutani[2],
E.J. Smith[2], R.D. Zwickl[3], and J.T. Gosling[4]

1 TRW Space and Technology Group, Redondo Beach, CA 90278

2 Jet Propulsion Laboratory, Pasadena, CA 91109

3 National Oceanic and Atmospheric Administration, Boulder, CO 80303-3328

4 Los Alamos National Laboratory, Los Alamos, NM 87545

Abstract

The plasma wave measurements obtained during ISEE-3's deep passes through the geomagnetic tail found that moderate to intense electric field turbulence occurred in association with the major plasma and magnetic field regions and flow phenomenae. In the magnetopause boundary layer, the electric field spectral amplitudes are typically sharply peaked at 316 Hz to 562 Hz. The tail lobe region which is upstream of slow shocks and is magnetically connected to the plasma sheet is characterized by wave spectra that peak in the 100 Hz-316 Hz range and at the electron plasma frequency. Within the plasma sheet, broadband electrostatic noise occurs in regions where the magnetic field strength exceeds 2 nT; this noise can also be found in the plasma sheet boundary layer in association with strong field-aligned plasma flows. As ISEE-3 moved between the different distant tail regions, distinct but often subtle changes occur in the plasma wave spectra. Occasionally, plasma oscillations indicate that the distant tail contains a population of relatively dense cold electrons.

Plasma Waves in the Distant Geomagnetic Tail

1. Introduction

Broadband electrostatic noise (BEN) is a nearly ubiquitous feature of the near earth plasma sheet boundary layer (Scarf et al, 1974; Gurnett et al, 1976; Grabbe and Eastman, 1984). In the distant geomagnetic tail, the initial ISEE-3 survey by Scarf et al (1984a) found that electrostatic wave activity in the 17.8 Hz to 10 kHz frequency range occurred in the magnetopause boundary layer and within the plasma sheet. In the upstream region of the three slow shocks discovered by Feldman et al (1984), Scarf et al (1984b) also detected narrowband electrostatic emissions (NEN) with peak frequencies between 100 to 316 Hz and higher frequency electron plasma oscillations. Similar electrostatic noise was detected inside magnetotail flux ropes (Kennel et al, 1986).

The purpose of this paper is simply to document the behavior and spectral characteristics of the distant tail electrostatic emissions. In section 2-6, we present five events which include ISEE-3 encounters with plasmoids, slow shocks, the plasma sheet boundary layer with strong field-aligned plasma flows, the central plasma sheet, and the magnetopause boundary layer and/or plasma mantle. The particle and magnetic field aspects of some of these events have been previously discussed in the literature. We find that the plasma waves observed in each of these regions have distinct spectral properties, although the changes which occur as ISEE-3 passes from one region to another are often quite subtle. We also find evidence that the distant tail can occasionally contain a dense population of cold electrons. Section 7 summarizes the observed wave properties and comments on some

of the perplexing issues raised by the impulsive temporal behavior of the emissions and their occurrence over large spatial regions.

2. January 27, 1983

Figure 1 displays the ISEE-3 encounter with the plasma sheet between 0230 UT and 0315 UT on January 27, 1983, when the spacecraft was approximately 214 R_E behind the earth. The top four panels show the three-second average magnitude and three solar ecliptic components of the magnetic field measured by the JPL magnetometer (Frandsen et al, 1978). The lower panels exhibit the calibrated electric field spectral amplitudes (volts/meter - $(Hz)^{1/2}$) for frequency channels from 31 Hz to 10 kHz measured by the TRW/U. Iowa plasma wave detector; the electric field is obtained every 0.5 second, and the displayed wave data are unaveraged. Figure 2a shows the 90-second averaged electron density (n), temperature (T), and the flow speed (V), measured by the LANL plasma detector (Bame et al, 1978); unless otherwise indicated, all plasma flows are tailward. This event has previously been studied by several groups. Feldman et al (1985) identified the exit of the plasma sheet at 0301 UT as a slow shock with Alfven Mach number of 0.2, which is nearly the switch-off shock limit. Tsurutani et al (1985) interpreted the 0.1 Hz, quasi-transverse magnetic oscillations observed from 0242 UT to 0247 UT as right-hand magnetosonic waves driven unstable by a field-aligned energetic ion beam. Based on the bipolar B_Z signature and energetic ion measurements, Richardson and Cowley (1985) identified the plasma sheet entry at 0252 UT as a plasmoid.

The January 27, 1983 event exhibits all of the basic plasma wave properties which are associated with the plasma sheet in the distant

tail. Prior to the arrival of the plasmoid and energetic particles, ISEE-3 detected a moderately intense wave emission near 0231-32 UT. The magnetic field was steady and quiet with a magnitude of about 8 nT. The plasma flow speed was low ($V \leq 200$ km/sec), and the density was $n = 0.08$ em^{-3}, which is typical of the density in the distant tail lobes (Zwickl, et al, 1984). Figure 3 displays selected electric field amplitude spectra for this event; the lower curve is a one-minute average spectrum starting at the indicated time, and the top curve is the peak amplitude detected in each frequency channel (17.8 Hz to 100 kHz) during that minute. The average spectrum exhibits a peak between frequencies $f = 100$ and 178 Hz, which corresponds to $f/f_p = 0.04$-0.07 where $f_p = 9\sqrt{n}$ kHz is the electron plasma frequency. The average amplitudes at 17.8, 31, and 560 Hz are at the instrument threshold. The impulsive nature of the emission is indicated by the high peak-to-average ratio of 10. These low frequency emissions resemble the waves reported by Scarf et al (1984b) upstream of slow shocks on tail field lines which are connected to the plasma sheet nearer the earth. The slight enhancement from 3.11 kHz to 17.8 kHz represents weak continuum radiation which has a cut-off at the local electron plasma frequency ($f_p \approx 2.5$ kHz for $n = 0.08$ cm^{-3}).

The first indication of the coming plasmoid is the abrupt onset of strong electron plasma oscillations at about 0236 UT. The 0237 UT spectrum in Figure 3 shows a narrow peak at 3.16 kHz, the channel which is nearest to the $f_p \approx 2.5$ kHz value obtained from the electron density. In the ISEE-3 spectra, electron plasma wave activity is nearly always distinguished by a sharp, narrow spectral peak; since the channel filters are about 15% wide, strong plasma oscillations

will produce a response in the frequency channels which are adjacent to the channel nearest f_p. The electron plasma waves are probably excited by the classic "bump-on-tail" instability from energetic electrons which are streaming along the magnetic field lines connected to the near earth reconnection region.

At 0240:30 UT (0241:45 UT), enhanced fluxes of 91-147 keV (35-56 keV) ions arrived at ISEE-3, stimulating the growth of the right-hand magnetic oscillations (Tsurutani et al, 1985). At 0244 UT, the plasma flow velocity increased to about 350 km/sec, and new component of plasma wave activity developed between 31 Hz and 316 Hz. These emissions were quite strong with peak amplitudes at low frequencies near 10^{-4} v/m-$\sqrt{Hz}$. The 0244 UT spectrum below 178 Hz is essentially identical to the very intense BEN spectrum obtained by Gurnett et al (1978) on IMP-8 at 34 R_E in the near earth plasma sheet. However, unlike BEN, the spectrum falls rapidly above 178 Hz and does not extend to the electron plasma frequency. The low frequency emissions dominate until about 0250 UT, although their spectral shape is variable; the spectrum at 0247 UT has a weak maximum at 100 Hz due to a strong burst at this frequency between 0247 and 0248 UT.

At 0250-51 UT, the magnetometer detects the characteristic positive B_z signature of the tailward moving plasmoid. The E-field spectrum broadens in frequency to 3.16 kHz and becomes a smooth power law. The average wave amplitudes and spectral shape are very similar to the BEN spectrum shown by Grabbe and Eastman (1984), if their spectrum is sampled at the ISEE-3 channel frequencies. As the satellite enters the plasma sheet, the flow velocity increases from 400 km/sec at 0250 UT to over 10^3 km/sec at 0255 UT. At 0252 UT, the

magnetic field reaches a local minimum of 2 nT, and the plasma waves essentially disappear. The absence of plasma wave emissions within the central low magnetic field (<2 nT) region of the plasma sheet, which also occurs between 0258 to 0300 UT, is typical of the near earth central plasma sheet (Gurnett et al, 1976).

From 0253 UT to 0258 UT, the magnetic field strength decreases from nearly the lobe value (~8 nT) to an intermediate value of 4 nT. The E-field spectrum is very broad with an irregular power law shape; the intense emissions extend up to 3.16 kHz. During this intense interval, the LANL electron density varies between n = 0.04 to 0.064 cm^{-3}, which implies that the electron plasma frequency is in the range f_p = 1.8 to 2.3 kHz. The 0254 UT spectrum does not exhibit a sharp peak in any of the channels near f_p, as almost always occurs for electron plasma oscillations. The maximum Doppler shift for a wave with wave vector K is $\Delta f = KV/2\pi = f_p\ (V/V_T)\ K\lambda_D$ where $V_T = (T_e/m)^{1/2}$ and $\lambda_D = V_T/\omega_p$ is the Debye length. For the measured electron temperature of $T_e = 2.6 \times 10^6$ °K and f_p = 1.8 to 2.7 kHz, we find for the maximum how speed $V = 10^8$ cm/sec Δf = 0.3-0.44 $K\lambda_D$ kHz, which is clearly insufficient to Doppler shift the low frequency waves up to 3.16 kHz. Doppler shifting could smear a weak f_p (~2 kHz) emission into adjacent frequency channels (1.0 and 3.16 kHz), although the absence of a peak in the 1.78 kHz argues against this interpretation of the high frequency spectrum. Alternatively, the broad frequency spectrum might result from a combination of different instabilities as is thought to occur in near earth BEN (Grabbe, 1987; Schriver and Ashour-Abdalla, 1987).

The ISEE-3 exit from the plasma sheet between 0300 and 0302 UT was

identified by Feldman et al (1985) as a slow shock. Across the shock, the density (temperature) changed from 0.08 cm^{-3} (2.7 x 10^6 ^oK) downstream to 0.08 cm^{-3} (9 x 10^5 ^oK) upstream (Schwartz et al, 1987). However, immediately after the data gap (0302-0303:40), the density increased as the temperature continued to decline, while the tailward flow speed remained in the range 300 to 500 km/sec until 0308 UT. The E-field spectrum at 0303:40 UT is a power law at low frequencies and a clear plasma oscillation peak at 1.78 kHz (f_p = 2 kHz for n = 0.05 cm^{-3}). The low frequency spectrum resembles the intense low frequency emissions detected between 0244-0248 UT, indicating the essential symmetry of the pre- and post-plasma sheet encounter regions. From 0304 to 0308 UT, the plasma oscillations increase in frequency (1.78 kHz to near 5.6 kHz), which is consistent with the observed increase in electron density.

At 0307:30 UT, the >35 keV ion fluxes decreased rapidly to the pre-plasmoid level. The plasma flow speed dropped to ~200 km/sec and plasma oscillations disappeared, suggesting that the plasmoid associated conditions ceased at this time. In the next few minutes, the plasma density increased to nearly 0.5 cm^{-3}, the electron temperature declined to 4 x 10^5 ^oK, and weak bidirectional fluxes of suprathermal electrons were observed on the LANL color spectrograms (not shown). These plasma characteristics indicate that after 0308 UT ISEE-3 entered the boundary layer region of the tail lobes in which the field lines are connected to the earth and are open to the solar wind (Baker et al, 1986). The intense low frequency plasma waves which develop after 0308 UT have a broad spectral peak near the 178-316 Hz and resemble the tail boundary layer emissions first reported

by Scarf et al (1984a).

The January 27 plasmoid event exhibits the variety of plasma wave phenomena detected in the different regions of the distant tail. On tail field lines which connect to the plasma sheet nearer the earth, i.e., reconnected field lines, there occurred a narrowband electrostatic emission with peak frequencies near 100-178 Hz which had previously been reported in the region upstream of slow shocks (Scarf et al, 1984b). Preceding the arrival of the plasmoid associated energetic ions are very intense electron plasma oscillations which are presumably destabilized by field-aligned beams of energetic electrons. Within the plasma sheet boundary layer containing the right-hand magnetosonic waves, a new intense to low frequency emission was observed which is highly impulsive and has a steep power law-like spectrum that only extends to about 560 Hz. The moderately magnetized ($B > 2$ nT) plasma sheet contains a broadband emission with a power law spectrum extending up to the electron plasma frequency. Finally, in the tail boundary layer, the wave emissions exhibit a peaked spectrum near 178-316 Hz. Both the impulsive nature and spectrum of these waves resemble the narrowband noise observed on tail field lines upstream of slow shocks; however, the plasma conditions and magnetic connectivity of the boundary layer and upstream lobe region are very different, which suggests that the two emissions may have different sources.

3. February 4, 1983

Figure 4 displays the magnetic field and plasma wave measurements from 0530 to 0630 UT on February 4, 1983. During this interval, Richardson and Cowley (1985) have identified two plasmoid events from

0542-0555 UT and 0617-0627 UT. The 0540 UT entrance into the plasma sheet possesses the expected characteristics of a slow shock but was not so identified by Feldman et al (1985). Weak >35 keV proton fluxes (not shown) were observed only within the plasma sheet-plasmoid encounters (0538 to 0600 UT and after 0612 UT).

From 0530 to 0538 UT, the LANL electron detector measured a steady tailward flow velocity of 150-200 km/sec, a plasma density of 0.4 cm^{-3} which slowly decreased in time, and an electron temperature of 6 x 10^5 ^0K which slowly increased in time. The LANL color spectrograms (not shown) exhibit a weak bidirectional flux of suprathermal electrons which persisted until about 0537 UT. Thus, the plasma characteristis identify the 0530 to 0534 UT interval as the tail boundary layer or possibly the plasma mantle (Bame et al, 1983; Baker et al, 1986). Intense plasma wave turbulence with a spectral peak at 316 Hz (Figure 5) occurred throughout this interval which is typical of tail boundary layer emissions.

At 0538 UT, about one minute before plasma sheet entry, the plasma flow speed increased to 450 km/sec, and a subtle change occurred in the wave emissions. The low frequency noise from 56 Hz to 178 Hz sharply increased as the intensity of the 562 Hz channel diminished; in addition, a weak emission commenced in the high frequency 1.78 kHz to 5.62 kHz channels. The average low frequency spectrum exhibited a broad peak with the largest signals occurring at 100 Hz. This change in wave properties, the onset of plasma flow, and the cessation of bidirectional electron fluxes after 0537 UT indicates that during the brief interval between 0538 UT and the plasma sheet encounter at 0539 UT, ISEE-3 entered onto field lines which connected to the plasma

sheet.

Within the plasma sheet, the density increased to ~0.6 cm^{-3}, the electron temperature rose to ~1.2 x 10^6 ^oK, and the plasma flow speed varied between 350 and 650 km/sec. The plasma wave spectrum was a broadband power law which extended up to at least 5.62 kHz (see 0543:44 UT spectrum) except near the weak field regions near 0546 UT and 0548 UT where the wave amplitudes were near background.

Near 0550 UT, ISEE-3 left the plasma sheet and entered the plasma sheet boundary layer. For the next nine minutes, the plasma density, electron temperature, and flow speed gradually decreased as the magnetic field slowly increased toward the lobe value of ~10 nT. Very impulsive low frequency plasma noise occurred throughout this interval, with one burst near 0555 UT reaching a peak of 10^{-3} v/m - $(Hz)^{1/2}$ at 178 Hz (see 0557:48 UT spectrum in Figure 5). Just after 0559 UT, another subtle change occurred in the plasma and wave characteristics. The plasma density (temperature) became steady at 0.2 cm^{-3} (8 x 10^5 ^oK), and the plasma flow speed varied slightly between 200 and 250 km/sec. Energetic proton fluxes (not shown) diminished to low values and weak bidirectional fluxes of suprathermal electrons appeared. Although still impulsive, the 100 to 316 Hz plasma waves achieved a steadier and lower peak amplitude. The 5.62 kHz channel exhibited a weak peak (see 0600:52 UT spectrum, Figure 5), indicating low level plasma oscillation activity. These combined changes indicate that between 0559 and 0612 UT ISEE-3 was once again within the tail boundary layer region.

After 0612 UT, ISEE-3 encountered a magnetically complex plasmoid. As the positive B_Z signature of the plasmoid developed, B_y first

became slightly negative (B_y = -4 nT at 0618 UT), then sharply rotated to +4 nT, and finally switched to nearly -8 nT at 0619 UT as B_z began to decrease toward zero. Although the positive B_z portion of the plasmoid reached nearly +10 nT, the trailing edge of the plasmoid had only a negative B_z (~ -2 nT) which occurred mostly after the spacecraft began to exit the plasma sheet at 0627 UT. At the leading edge of the plasmoid (0612 UT), energetic proton fluxes suddenly appeared, the plasma flow speed jumped to 400 km/sec, the bidirectional suprathermal electron fluxes disappeared, and the wave intensity sharply decreased. As the field strength and $|B_x|$ decreased after 0614:30 UT, an intense burst of plasma waves occurred at 178-316 Hz; although the 0615:25 UT spectrum in Figure 5 is similar in shape to the 0606:21 UT spectrum measured in the tail boundary layer, the average and peak amplitude are significantly higher. Upon entering the plasma sheet, the wave intensity diminished but became very broadband, extending from 17 Hz to 5.6 kHz in a power law spectrum (not shown). At 0626 UT, the spacecraft entered the plasma sheet boundary layer and encountered very strong plasma wave turbulence with a broad peak between 56 and 178 Hz (see the 0628:31 UT spectrum).

The February 4 event exhibits the distinct, but sometimes subtle, changes which occur in the plasma wave spectra as the spacecraft moves into different regions of the distant tail. In the tail boundary layer (or mantle), the wave spectra peak at mid-frequencies (316 to 562 Hz) with very little amplitude at low frequencies ($\lesssim$100 Hz); although temporally impulsive, the peak amplitudes are roughly constant from burst to burst. On lobe field lines which are just adjacent and connect to the plasma sheet, the spectral peak shifts

downward to 100-316 Hz, and the low frequency (<100 Hz) amplitudes are enhanced; the peak amplitudes are highly variable and occasionally reach very large values.

4. February 7, 1983

Figure 6 presents magnetic field and plasma wave measurements from 1215 UT to 1300 UT on February 7, 1983. The field magnitude shows two clear encounters with the plasma sheet. ISEE-3 entered the plasma sheet from the southern lobe at 1221 UT and exited into the southern plasma sheet boundary layer at 1224 UT. The spacecraft remained in the boundary layer, measuring a persistent 550 km/sec tailward flow, until 1236 UT, when it rapidly reentered the sheet. Feldman et al (1985) identified this entry as a slow shock. However, their listed density and electron temperature changes do not agree with the LANL measurements shown in Figure 2; the tailward flow velocity did increase from 550 km/sec to 10^3 km/sec at this time. At about 1240 UT, the satellite exited the plasma sheet and measured a sharp decrease in the flow speed; the observed density and electron temperature decreases do correspond to the values given by Feldman et al (1985) for the slow shock. The apparent discrepancy between the quoted shock time and the observed plasma changes is probably not significant for our discussion. The plasma sheet entry (exit) at 1221 UT (1240 UT) occurred in coincidence with a sharp increase (decrease) in flow speed, and the flow was enhanced throughout the interval. Hence, the entry and exit possess the velocity characteristics of a slow shock, and the high flow speed measured in the plasma sheet boundary layer indicates that ISEE-3 remained in contact with the rapidly flowing plasma sheet.

In the few minutes prior to 1215 UT, the plasma density (electron temperature) was ~0.08 cm^{-3} (8 x 10^5 ^oK) which indicates that the ISEE-3 was on lobe field lines. The plasma wave spectra exhibited peaks at 100-178 Hz and at 1.78-3.16 kHz near the electron plasma frequency; these spectra are characteristic of the region upstream of slow shocks on field lines which connect to the plasma sheet. By 1216 UT, the earlier low frequency peaks and plasma oscillations have disappeared, and at 1217 UT, a new intense emission developed at 316-562 Hz (see the 1218 UT spectrum in Figure 7) with little power at lower frequencies (<100 Hz). The wave spectrum, the simultaneous increase in plasma density to 0.2 cm^{-3}, and the magnetic field strength indicate that ISEE-3 entered a different tail region which is probably either the plasma mantle or tail boundary layer. At 1219 UT, the field strength decreased slightly, the density dropped to 0.1 cm^{-3}, and the wave spectrum changed to a low amplitude power law extending to low frequencies which persisted as ISEE-3 entered the plasma sheet at 1220 UT (see the 1221 UT spectrum in Figure 7). These distinct changes in the wave spectra indicate that at 1219 UT the spacecraft reentered the tail lobe or plasma sheet boundary layer.

Upon entering the plasma sheet boundary layer at 1224 UT, the low frequency wave intensified, and a gentle spectral peak at 100 Hz developed and persisted (the 1225 UT and 1232 UT spectra in Figure 7). Although the peak is less pronounced, these spectra resemble those observed upstream of slow shocks; the impulsive and highly variable peak amplitudes are also consistent with this interpretation. However, unlike the upstream slow shock spectra which fell rapidly at frequencies above the peak, the wave activity after 1224 UT extends to

3.11 kHz and resembles the broadband emissions detected in the plasma sheet. The low plasma density of 0.09 cm^{-3} measured during the 1224 UT to 1236 UT interval indicates that the plasma sheet boundary layer field lines connect to the low density lobe region encountered prior to 1215 UT. The relatively high flow velocity (~550 km/sec) observed during this interval suggests that the spacecraft did not penetrate completely through the slow shock layer into the lobe, but remained near the outer layer or leading edge of the slow shock transition (shock-heated and rapidly flowing (~800-1,000 km/sec) downstream protons should penetrate to the leading edge of the shock).

At 1235 UT, the wave spectrum abruptly changed from a weak 100 Hz peaked spectrum to a power law. The satellite then quickly entered the plasma sheet, and the wave activity disappeared as the magnetic field strength dropped to below 2 nT. Across the abrupt field decrease, the density jumped from 0.09 cm^{-3} to 0.2 cm^{-3}, the electron temperature increased from 10^6 °K to 2 x 10^6 °K, and the flow speed gradually rose from 550 km/sec to 1,000 km/sec. Within the plasma sheet, weak broadband wave activity returned at 1238 UT as the field strength increased above 2 nT. Near 1240 UT, the magnetic field increased to values slightly above those of the earlier plasma sheet boundary layer interval, and the plasma wave levels and spectral shape returned to those characteristic of the boundary layer (compare the 1241 UT and 1225 UT spectra in Figure 7).

From 1244:54 to 1246 UT, a short burst of electron plasma oscillations at 5.62 kHz occurred just as ISEE-3 entered the smooth magnetic field region of the tail lobes. At this time, wave activity below 100 Hz diminished, leaving a broad peaked spectrum at mid-

frequencies (1245 UT spectrum in Figure 7), the plasma density increased from 0.1 cm^{-3} to 0.2 cm^{-3}, and the tailward flow speed dropped from 750 km/sec to about 200 km/sec. Energetic proton fluxes (not shown), which had been present since 1215 UT, also decreased sharply at 1246 UT. Between 1246 UT and 1255 UT, weak bidirectional fluxes of energetic electrons were observed. Taken together, these measurements indicate that from 1246 to 1255 UT ISEE-3 was in the magnetopause boundary layer. At 1255 UT, a burst of 5.62 kHz plasma oscillations and a decrease of density to ~0.12 and subsequently to 0.08 at 1258 UT indicated that the spacecraft reentered the tail lobe field lines which connect to the plasma sheet.

The February 7 event again demonstrates that distinct changes occur in the plasma wave properties when the spacecraft enters or leaves a tail plasma region. Of particular interest is the plasma sheet boundary layer interval (1224-1236) in which the wave spectra exhibited a mixture of the peaked spectrum typically observed upstream of slow shocks and the broadband spectrum detected in the moderately magnetized regions of the plasma sheet. The plasma flow speed was intermediate (~500 km/sec) between the high speed flow in the central plasma sheet and the low speed (or zero) flow usually detected upstream of slow shocks. The observations suggest that during the 1224-1236 UT, period ISEE-3 sampled the leading edge of the plasma sheet slow shocks.

5. February 10, 1983

A plasma sheet encounter with a somewhat different flow morphology occurred from 0300 to 0400 UT on February 10, 1989 (Figure 8). This event is not listed as either a slow shock or a plasmoid; however,

strong auroral kilometric radiation (not shown) was detected by ISEE-3 from about 0015 to 0130 and from 0215 to 0340 UT, indicating the occurrence of the intense substorms. The first substorm produced a clear plasmoid B_z and flow signature at 0100 UT. The 0300 UT event does exhibit a weak B_z deflection near 0312 UT which may represent the passage of a plasmoid.

At 0300 UT, ISEE-3 was in the southern tail lobe and measured a typical lobe density (temperature) of 0.08 cm^{-3} (6 x 10^5 ^oK) and low flow speed. Just after 0305 UT, a weak electron plasma oscillation emission at 5.6 kHz begin to intensify, and at 0305 UT, the satellite detected enhanced fluxes of energetic protons (>35 keV) and the onset of magnetosonic waves. By 0308 UT, strong mid-frequency E-field turbulence had developed which initially (0309:04 UT spectrum in Figure 9) exhibited a distinct peak at 178 Hz. As the spacecraft entered the outer boundary layer of the plasma sheet, the magnetosonic waves disappeared, a strong tailward flow commenced, and the wave spectrum changed to a power law shape (0311:05 UT spectrum in Figure 9). The entry to (exit from) the plasma sheet at 0316 UT (0322 UT) was marked by an intense broadband wave burst; similar strong emissions occurred within the moderately magnetized region of the plasma sheet.

After leaving the plasma sheet, the plasma flow speed did not diminish but remained high until after 0400 UT. Magnetosonic waves, electron plasma oscillations, and broadband low frequency wave turbulence persisted throughout this interval. At 0325 UT (Figure 8), the wave spectrum developed a unique low frequency peak at 100 Hz which lasted for the next three minutes. By 0328 UT, the wave

spectrum returned to the familiar broad peak, which then persisted to 0400 UT; however, the peak frequency gradually increased from 178 Hz (0330 UT) to 178-316 Hz (0348 UT) to 562 Hz (0358 UT).

During this interval, the frequency of electron plasma oscillations increased from 3.16 kHz (0325 UT) to between 3.16 and 5.6 kHz (0330 UT), to 5.6 kHz (0348 UT) and finally to 10 kHz (0358 UT). This upward movement of the electron plasma frequency is apparent in Figure 8 as the peak amplitudes in the high frequency channels change from 3.11 kHz to 10 kHz. This upward progression is not monotonic in time; at 0352 UT, f_p jumps from 5.6 kHz to 10 kHz, returns to 5.6 kHz at 0354 UT, and then finally settles at 10 kHz after 0358 UT. The observed rise in the electron plasma frequency corresponds to an increase in the total electron density from ~0.1 cm^{-3} at 0324 UT to ~1.0 cm^{-3} at 0400 UT. Interestingly, the electron density reported by the LANL plasma instrument (Figure 2) was essentially constant at ~0.1 cm^{-3} from 0328 UT to 0400 UT. Normally, our determination of the electron density by using electron plasma oscillations is in excellent agreement with the LANL density measurements, as occurs for this event at 0325 UT. Thus, we suggest that the observed plasma frequency line at 10 kHz does indeed indicate a total electron density near 1.0 cm^{-3} and that the difference between our inferred and LANL's reported density is due to the presence of cold electrons with energies near or below the threshold of the LANL instruments. R. Zwickl (private communication) has found that the LANL processing routines will occasionally miss low energy contributions to the electron distribution function and thus report a total density which is too low.

In summary, the February 10 event exhibits several features which

resemble spacecraft encounters with the near earth plasma sheet. Strong tailward field-aligned flow persisted in the plasma sheet boundary layer for over 36 minutes after the ISEE-3 left the sheet. Similar long duration field-aligned flows are commonly observed near the earth with the flow direction, however, typically being earthward (Decoster and Frank, 1979). Broadband electrostatic noise also occurred throughout the boundary layer as in the near earth plasma sheet (Grabbe and Eastman, 1984). Although the wave spectrum typically exhibited a peak in the range 178-562 Hz, the wave emissions did extend up to the electron plasma frequency. Finally, the plasma oscillations yielded evidence that cold electrons with order one densities can occasionally be present in the distant tail. L. Frank (private communication) has found similar high densities of cold electrons, apparently of ionospheric origin, to occasionally be present in the near earth plasma sheet boundary layer.

6. March 25, 1983

Figure 10a and 10b display the magnetic field and plasma wave measurements obtained on March 25, 1983, from 0800 UT to 0930 UT when ISEE-3 was located at about 100 R_E downstream. These two plasma sheet crossings at 0824 UT and 0902 UT are part of the CDAW-8 data set and have been discussed by Fairfield et al (1988). The earlier (0713 UT) plasma sheet encounter was analyzed in terms of a magnetic flux rope by Sibeck et al (1984) but has recently been reinterpreted as a two-loop plasmoid by Richardson et al (1988). Fairfield et al (1989) noted that a substorm onset occurred near local midnight at 0750 UT and that a minor intensification developed at 0923 UT. Richardson et al (1988) questioned the earlier interpretation of the 0824 UT plasma sheet

crossing as a plasmoid (Richardson and Cowley, 1985) due to the weak B_z variations. Fairfield et al (1988) suggested that the 0824-0848 UT interval may represent a sequence of small plasmoids.

At 0800 UT, ISEE-3 was in the northern tail lobe and measured a strong magnetic field of 22 nT. The electron density was ~0.4 cm^{-3}, the electron temperature was ~2 x 10^5 °K, and the plasma flow was 100-150 km/sec tailward. The high density, low temperature, and moderate flow speed are consistent with the spacecraft being in the plasma mantle (Bame et al, 1983) which probably filled the tail lobes on this geomagnetically active day. The E-field channels exhibit moderate intensity mid-frequency noise which peaks between 316 and 562 Hz (Figure 11) and is near background below 178 Hz; this noise has an essentially identical spectrum to the emissions observed in the moderately dense (~0.3 cm^{-7}) magnetopause boundary layer and/or plasma mantle in the distant tail. The 5.6 kHz channel shows a slight enhancement of the average amplitude which the 0807 UT spectrum in Figure 11 demonstrates is the low frequency cut-off of the continuum radiation; weak plasma oscillations appear to be superposed on the average wave level, thus confirming that the plasma density is ~0.3-0.4 cm^{-3}.

As the precursor of the advancing plasmoid, the 75-115 keV electron flux (not shown) increased sharply at 0811 UT and was followed by similarly rapid flux increases of 112-157 protons at ~0813 UT and 30-36 keV protons at ~0816 UT (Scholer et al, 1984). The arrival of the energetic electrons was nearly simultaneous with the onset of strong 5.6 kHz electron plasma oscillations and of low frequency ($\lesssim$100 Hz) waves. (Recall that the January 27 plasmoid event

had a very similar wave-particle morphology.) At 0814 UT, the 316 Hz channel, and to a lesser extent the 178 Hz channel, develops an unusual emission in which the wave amplitude becomes almost steady in time rather than the more typical temporally impulsive signals. The 0816 UT spectrum in Figure 11 exhibits a sharp narrow peak at 316 Hz. In the right-hand panel of Figure 11, we also display the magnetic amplitude spectrum ($nT/\sqrt{Hz}$) which shows an intense narrowband emission that peaks at 316 Hz and has significant power down to 100 Hz. Since the electron cyclotron frequency is ~620 Hz, these magnetic waves are propagating in the whistler mode.

In our experience, intense whistler mode emissions are extremely rare in the distant tail. The only other documented observance of whistlers also occurred on March 25 near 0718 UT, which is the center of the Sibeck et al (1984) flux rope event (Kennel et al, 1986). The amplitude and shape of both the mid-frequency E-field and B-field spectra at the 0718 UT and 0816 UT are nearly identical. Kennel et al (1986) demonstrated that for the 0718 UT event the B-to-E amplitude ratio was consistent with the whistler dispersion relation. For the 0816 UT emission, the index of refraction for parallel whistlers at 316 Hz (178 Hz) is 17 (18.8). In terms of the electric and magnetic wave amplitudes, the refractive index should be approximately equal to 0.3B(nT)/E(v/m); the index of refraction inferred from the measured wave amplitudes is 30 (34) for the average 316 Hz (178 Hz) wave amplitudes and is 18 for both 316 Hz and 178 Hz using the peak amplitudes. Hence, the electric and magnetic amplitudes are consistent with a whistler mode interpretation. Interestingly, the previous spectrum (not shown) at 0815 UT shows no magnetic signal (it is

identical to the 0807 UT magnetic spectrum which is the instrument threshold) while the E-field spectrum has the same shape as at 0816 UT but with an average (peak) amplitude at 316 Hz which is 2.5 (3.3) times lower. Since the 0816 UT 316 Hz average amplitude is 25 times above the instrument threshold, the observed 0815 UT 316 Hz E-field amplitude is far above that expected ir the only signal in this channel was due to whistlers. Hence, the 316 Hz signal at 0816 UT probably consists of both electrostatic and electromagnetic emissions.

After 0816 UT, the whistler magnetic signals continued with a peak near 178-316 Hz while the mid-frequency E-field spectra broadened to lower frequencies (see the 0820 UT spectrum). The 316 Hz E and B amplitudes remained consistent with the expected whistler index of refraction; however, at 100 Hz, the index inferred from the B-to-E ratio was six times smaller than expected, indicating that the waves were predominantly electrostatic. In addition, the E-field amplitudes in all channels exhibit the characteristic impulsive behavior after 0818 UT, although the minima in the 316 Hz channel remain above the instrument threshold.

Near 0825 UT, tailward plasma flow starts at speeds ~400 km/sec and approaches 900-1,000 km/sec by 0830 UT. ISEE-3's entrance into the plasma sheet is magnetically very turbulent with large excursions of the field in both B_y and B_z. Near the edge of the current sheet (0827 UT), the E-field spectrum has become a broadband power law extending up to 10 kHz. The earlier B-field emission at 178-316 Hz has nearly disappeared and been replaced by a low frequency (17 and 31 Hz) falling spectrum; whistler emissions between 100-178 Hz reappear at 0828 UT and at 0832 UT during local maxima (or plateau's) in the

magnetic field strength.

An interesting magnetic structure occurred 0834:30 to 0836 UT. B_X was approximately zero as the spacecraft was about to cross into the southern lobe. However, B_y and B_z become fairly steady with values of B_y = -11 nT and B_z = 9 nT, thus accounting for the 16 nT peak in total B. This very unusual field orientation occurred while the plasma flow was strongly tailward and clearly suggests the tailward convection of some type of coherent flux bundle; the local Alfven speed was probably of order 600-700 km/sec so that the flow velocity may have exceeded the Alfven speed. During the passage of the flux tube, the E-field emissions were quite different from those in the surrounding plasma sheet; although still impulsive and with a power law shape, the minimum amplitudes were significantly elevated above background. The B-field spectra, however, exhibited little change from 0832 UT to 0839 UT, all more or less resembling the 0835 UT spectrum shown in Figure 11. From 0837 to 0838, a similar appearing local maxima in the magnetic field occurred; however, this increase was in B_X and was apparently caused by an excursion toward the southern lobe.

At 0840 UT, ISEE-3 abruptly exited the plasma sheet and entered the boundary layer where the field strength was about 18 nT, slightly less than in the lobes. The flow speed decreased to 600 km/sec tailward, exhibited a brief earthward burst at 0842 UT and then decreased to ~150 km/sec as the spacecraft entered the lobes near 0844 UT. Within the plasma sheet boundary layer, the E-field was very intense with peak amplitudes reaching 10^{-3} v/m - $(Hz)^{1/2}$. The wave spectrum was strongly peaked at 178 Hz and extended to low frequencies, which is typical of the peaked boundary layer wave

emissions observed upstream of slow shocks. However, the magnetic field strength during the March 25 event was more than a factor of two larger than were the upstream field strength measured for the slow shocks discussed by Scarf et al (1984). Hence, the peak frequency of these slow shock-boundary layer emissions is apparently independent of the magnetic field strength.

Figure 10b displays the next 45 minutes of plasma wave and magnetic field measurements. From 0845 to 0902 UT, the moderate density (~0.3 cm^{-3}), the electron temperature (~7 x 10^5 ^oK), and the low flow speed indicate that ISEE-3 was in the mantle filled lobe or the edge of the plasma sheet boundary layer. The wave emissions indicate that the spacecraft remained magnetically connected to the plasma sheet for at least most of this interval. Distinct bursts of plasma oscillations at 5.6 kHz exhibited very abrupt onsets and cessations, suggesting an intermittent plasma sheet connection. The mid-frequency emissions (Figure 12) have the typical spectral peak which decreased from 316 Hz at 0846 UT to about 100 Hz at 0854 UT. At 0858:30 UT, a very intense burst of low frequency noise occurred whose general character and rapidly falling spectrum strongly resembles the 0244 UT low frequency emission on January 27.

Just after 0901 UT, ISEE-3 entered a rapidly flowing plasma sheet, and the wave spectrum broadened into a power law-like form which extended to 10 kHz. Near 0804 UT, the spacecraft crossed from the southern to the northern part of the tail. This crossing, however, was quite unusual since the magnetic field strength did not decrease below 10 nT. When B_X passed through zero, B_y (B_z) was -9 nT (+3.5 nT) which is similar to the field orientation within the earlier plasma sheet

crossing at 0835 UT. During a later plasma sheet crossing at 1038 UT (not shown), the field also did not decrease below 10 nT in magnitude and was oriented primarily in the negative y- direction at the B_x reversal (Fairfield et al, 1988). Shortly after 1100 UT, ISEE-3 briefly entered the magnetosheath and measured a southward and dawnward field. Hence, the field at the center of the plasma sheet for three successive crossings very likely had the same dawnward B_y orientation as the magnetosheath.

At 0915, ISEE-3 entered the plasma sheet boundary layer and remained there until 0920 UT when a sharp cessation of the 5.6 kHz plasma oscillations and the dropout of energetic protons (not shown) indicate that the spacecraft moved into the tail lobe. The electron parameters and the persistent mid-frequency wave emissions peaked at 316 Hz are consistent with the satellite being within the plasma mantle or magnetopause boundary layer.

7. Discussion

The above examples suggest that the wave emissions in the distant tail have distinct characteristics and associations. In the magnetopause boundary layer and/or plasma mantle, the E-field spectra are typically peaked near 316 to 562 Hz; the spectra decrease sharply to both lower and higher frequencies such that by 100 Hz and 1,000 Hz the amplitudes are near background. These waves may be related to the bidirectional electron distributions which are frequently observed within the boundary layer. On field lines which apparently connect to the plasma sheet but which are essentially of lobe strength and orientation, the wave emissions exhibit a spectral peak in the range 100 to 316 Hz; the spectral range varies from sharply peaked to a

gradual or gentle bump. The peak frequency is apparently independent of the magnetic field strength, being similar in events whose field magnitudes differed by over a factor of two. The waves usually occur during intervals of low bulk plasma flow. These emissions were first detected upstream of slow shocks and may be related to the similarly peaked magnetopause boundary layer waves; their lower peaked frequency may simply reflect the lower plasma density of the plasma sheet boundary layer and tail lobes relative to the higher density magnetopause boundary layer.

On two occasions (January 27 and March 25) just before entering or after leaving the plasma sheet, an intense low frequency emission was detected. The waves are characterized by a rapidly monotonically falling spectrum which reached background by 1 kHz. For the January 27 event, these emissions began during an interval of right-hand magnetosonic wave activity at the onset of tailward plasma flow associated with a plasmoid; for the March event, there were no hydromagnetic waves or plasma flows.

Broadband electrostatic noise (BEN) is ubiquitously observed within the plasma sheet and frequently detected at the outer boundary of the plasma sheet during intervals of field-aligned flow. The BEN spectrum is monotonically falling with a power law-like shape and usually extends to near or even slightly above the local plasma frequency. Within the plasma sheet, BEN occurs in regions where the magnetic field strength exceeds 2 nT and disappears at lower field values. The spectrum, amplitudes, and occurrence of distant tail BEN are essentially identical to the corresponding properties of near earth BEN.

Finally, electron plasma oscillations occur on lobe-like field lines which are connected to the plasma sheet and are associated with the arrival of energetic plasmoid electrons and lower energy electron heat fluxes upstream of slow shocks. The plasma oscillations terminate upon the spacecraft entering the plasma sheet. On February 10, the plasma oscillations occurred at a significantly higher frequency than the electron plasma frequency based on the LANL electron density measurements for the energy range 10 ev to 1 keV. Thus, the wave observations indicate that occasionally the distant tail contains a dense population of cold (<10 ev) electrons which are presumably of ionospheric origin.

The absence of complete electron and ion measurements on ISEE-3 implies that we cannot determine whether the above wave emissions are uniquely associated with particular features in the particle distribution functions. Since the distant tail BEN occurs during intervals of plasma flow, the waves could be excited by the same ion beam instabilities--ion acoustic, beam resonant, and electron acoustic (Grabbe, 1987; Schriver and Ashour-Abdalla, 1987)--which are believed to generate BEN in the near earth plasma sheet. The spectrally peaked emissions, which can be called narrowband electrostatic noise (NEN), that occur upstream of slow shocks and in the magnetopause boundary layer are not associated with rapidly flowing plasmas. Unlike the near earth plasma sheet boundary layer, these regions probably do not contain dense ion beams since, if these beams did exist, the electrons would have exhibited significant parallel flow speeds in order to maintain a zero net current. Thus, NEN probably does not propagate as an ion beam mode. Recently, Coroniti and Ashour-Abdalla (1989)

suggested that slow shock-associated NEN represents a nonstandard plasma mode which results from a velocity space hole in the low energy electron distribution; the mode can be destabilized by either a positive slope in the electrons and/or a low density, hot, fast ion parallel ion beam. Whether the magnetopause boundary layer NEN represents a similar nonstandard mode is unclear.

A general feature of the lower frequency emissions in the distant tail is their impulsive behavior. The E-field amplitudes can rise from background to maximum and return to background on time scales of order one-half second (the ISEE-3 wave instrument resolution) to several seconds. The peak-to-average amplitude ratios are typically in the range 10 to 30. When combined with their widespread spatial occurrence, the impulsive nature of these emissions poses an interesting conundrum.

For the various instabilities which are thought to generate BEN and NEN, the growth rates (γ) are usually of order $\gamma/\omega_p \sim 1\text{-}5 \times 10^{-3}$. In the distant tail, the thermal fluctuation level for the electric field is about 10^{-8} volts/m-$\sqrt{\text{Hz}}$. The maximum electric field amplitudes are typically 5-10 x 10^{-5} volts/m-$\sqrt{\text{Hz}}$, with occasional strong bursts reaching amplitudes a factor of 10 larger. Thus, if the waves grow from the thermal fluctuation level to saturation in a time t_s, the number of amplitude e-foldings is of order $\gamma t_s \sim 10$. For $f_p \sim$ 5.6 kHz and the above range of growth rates, the saturation times are $t_s \sim$ 0.06-0.3 seconds. On this time scale, even the thermal electrons only travel a distance $\lesssim 0.25\ R_E$ so that the wave-particle interactions are quite localized. The saturation wave energy densities correspond to

$$\sum_k \frac{|E_k|^2}{8\pi n T_e} \sim 1\text{-}4 \times 10^{-6}$$

Thus, the free energy source for instability is probably small and/or the particular features (cold electrons, velocity space hole) of the particle distributions which allow a normal mode to exist in the BEN and NEN frequency range are fragile and easily destroyed. In either case, we would expect the waves to grow on the 0.1-1.0 second time scale, saturate by nonlinearly removing the free energy or special conditions which permitted wave growth, and leave the plasma stable or marginally stable. Hence, a single, short duration wave burst is consistent with general theoretical expectations for a weak spatially localized instability.

The conundrum then is to explain why the waves are observed to occur as long sequences of short bursts which clearly extend over large spatial regions in the distant tail. Extensive spatial occurrence connotes a strong or robust source of free energy. For example, if the instability is driven by an ion beam, the quasilinear relaxation time would be quite long. The ion velocity space diffusion coefficient is approximately

$$D \sim \frac{e^2 E_\nu^2}{2m_i^2}$$

where E_ν is the spectral amplitude in esu/cm-$\sqrt{Hz}$. The time required to diffuse an ion thermal speed is $\tau_D \sim A_i^2/D(A_i^2 = 2T_i/m_i)$ which is roughly 10^3 seconds for distant tail parameters. During this time, a thermal ion (beam ion moving at the local Alfven speed) would travel 20 R_E (100 R_E). Thus, an ion source of free energy could be robust and could excite waves over a large spatial region.

The question then becomes, if the free energy source is strong, why is the saturation amplitude so small? One possibility is that the normal mode and/or the unstable modes exist only over a very narrow range of plasma parameters and wave normal angles. For example, the beam resonant instability studied by Schriver and Ashour-Abdalla (1987) occurs only in a very restricted range of propagation angles. In such cases, a very small change in wave normal angle, which could arise from scattering off other modes or refractive propagation due to inhomogeneities, could transfer the initially unstable mode to a stable region of wave number space. Thus, the wave growth could be terminated at modest amplitudes before the wave was sufficiently strong to destroy the available free energy. Once outside the unstable parameter region, the wave could damp, thus producing a burst-like time profile. Since the source of free energy remains, the above growth-damping cycle could be repeated many times throughout a large spatial region.

Acknowledgement

It is a pleasure to acknowledge many beneficial discussions with M. Ashour-Abdalla, C.F. Kennel, and S. Moses.

This research was partially supported at TRW by NASA under contract NAS 5-28703, at the Jet Propulsion Laboratory, California Institute of Technology, under contract with NASA, at Los Alamos National Laboratory under the auspices of the U.S. Department of Energy with support from NASA.

References

Baker, D.N., S.J. Bame, W.C. Feldman, J.T. Gosling, R.D. Zwickl, J.A. Slavin, and E.J. Smith, "Strong electron bidirectional anisotropies in the distant tail: ISEE 3 observations of polar rain," J. Geophys. Res., 91, 5637, 1986.

Bame, S.J., J.R. Asbridge, H.E. Felthauser, J.P. Glore, H.L. Hawk, and J. Chavez, "ISEE-C Solar wind plasma instrument," IEEE Trans. Geosci. Electron, GE-16, 160, 1978.

Bame, S.J., R.C. Anderson, J.R. Asbridge, D.N. Baker, W.C. Feldman, J.T. Gosling, E.W. Hones, Jr., D.J. McComas, and R.D. Zwickl, "Plasma regimes in the deep geomagnetic tail: ISEE 3," Geophys. Res. Lett., 10, 912-915, 1983.

Coroniti, F.V., and M. Ashour-Abdalla, "Electron velocity space hole modes and narrowband electrostatic noise in the distant tail," Geophys. Res. Lett., 16, 747, 1989.

DeCoster, R.J., and L.A. Frank, "Observations pertaining to the dynamics of the plasma sheet," J. Geophys. Res., 84, 5099, 1979.

Fairfield, D.H., D.N. Baker, J.D. Craven, R.C. Elphic, J.F. Fennell, L.A. Frank, I.G. Richardson, H.J. Singer, J.A. Slavin, B.T. Tsurutani, and R.D. Zwickl, "Substorms, plasmoids, flux ropes, and magnetotail flux loss on March 25, 1983: CDAW 8," NASA Goddard Space Flight Center preprint, September, 1988.

Feldman, W.C., S.J. Schwartz, S.J. Bame, D.N. Baker, J. Birn, J.T. Gosling, E.W. Hones, Jr., D.J. McComas, J.A. Slavin, E.J. Smith, and R.D. Zwickl, "Evidence for slow-mode shocks in the deep geomagnetic tail," Geophys. Res. Lett., 11, 599, 1984.

Feldman, W.C., D.N. Baker, S.J. Bame, J. Birn, J.T. Gosling, E.W.

Hones, Jr., and S.J. Schwartz, "Slow-mode shocks: A semipermanent feature of the distant geomagnetic tail," J. Geophys. Res., 90, 233, 1985.

Frandsen, A.M.A., V. Connor, J. Van Amersfoort, and E.J. Smith, "The ISEE-C vector helium magnetometer," IEEE Trans. Geosci. Electron, GE-16, 195, 1978.

Grabbe, C.L., and T.E. Eastman, "Generation of broadband electrostatic waves in the magnetotail," J. Geophys. Res., 89, 3865, 1984.

Grabbe, C.L., "Numerical study of the spectrum of broadband electrostatic noise in the magnetotail," J. Geophys. Res., 92, 1185, 1987.

Gurnett, D.A., L.A. Frank, and R.P. Lepping, "Plasma waves in the distant magnetotail," J. Geophys. Res., 81, 6059, 1976.

Kennel, C.F., F.V. Coroniti, and F.L. Scarf, "Plasma waves in magnetotail flux ropes," J. Geophys. Res., 91, 1424, 1986.

Richardson, I.G., and S.W.H. Cowley, "Plasmoid-associated energetic ion bursts in the deep geomagnetic tail: Properties of the boundary layer," J. Geophys. Res., 90, 12,133, 1985.

Richardson, I.G., C.J. Owen, S.W.H. cowley, A.B. Galvin, T.R. Sanderson, M. Scholer, J.A. Slavin, and R.D. Zwickl, "ISEE-3 observations during the CDAW-8 intervals: Case studies of the distant geomagnetic tail covering a wide range of geomagnetic activity," 1988.

Scarf, F.L., L.A. Frank, K.L. Ackerman, and R.P. Lepping, "Plasma wave turbulence at distant crossings of the plasma sheet boundaries and neutral sheet," Geophys. Res. Lett., 1, 189, 1974.

Scarf, F.L., F.V. Coroniti, C.F. Kennel, R.W. Fredricks, D.A. Gurnett, and E.J. Smith, "ISEE-3 wave measurements in the distant geomagnetic tail and boundary layer," Geophys. Res. Lett., 11, 335, 1984a.

Scarf, F.L., F.V. Coroniti, C.F. Kennel, E.J. Smith, J.A. Slavin, B.T. Tsurutani, S.J. Bame, and W.C. Feldman, "Plasma wave spectra near slow mode shocks in the distant magnetotail," Geophys. Res. Lett., 11, 1050, 1984b.

Scholer, M., G. Gloeckler, B. Klecker, F.M. Ipavich, D. Hovestadt, and E.J. Smith, "Fast moving plasma structures in the distant magnetotail," J. Geophys. Res., 89, 6717, 1984a.

Schriver, D., and M. Ashour-Abdalla, "Generation of high frequency broadband electrostatic noise: The role of cold electrons," J. Geophys. Res., 92, 5807, 1987.

Schwartz, S.J., M.F. Thomsen, W.C. Feldman, and F.J. Douglas, "Electron dynamics and potential jump across slow mode shocks," J. Geophys. Res., 92, 3165, 1987.

Sibeck, D.G., G.L. Siscoe, J.A. Slavin, E.J. Smith, S.J. Bame, and F.L. Scarf, "Magnetotail flux ropes," Geophys. Res. Lett., 11, 1090-1093, 1984.

Tsurutani, B.T., I.G. Richardson, R.M. Thorne, W. Butler, E.J. Smith, S.W.H. Cowley, S.P. Gary, S.I. Akasofu, and R.D. Zwickl, "Observation of the right-hand resonant ion beam instability in the distant plasma sheet boundary layer," J. Geophys. Res., 90, 12,159-12,172, 1985.

Zwickl, R.D., D.N. Baker, S.J. Bame, W.C. Feldman, J.T. Gosling, E.W. Hones, Jr., D.J. McComas, B.T. Tsurutani, and J.A. Slavin,

"Evolution of the earth's distant magnetotail: ISEE 3 electron plasma results," J. Geophys. Res., 89, 11,007, 1984.

Figure Captions

Figure 1 - The plasmoid and slow shock encounter on January 27, 1983. The top four panels display the three-second averaged magnitude and solar ecliptic components of the magnetic field. The lower panels display the 31 Hz to 10 kHz wave electric field spectral amplitudes (volts/m-$(Hz^{1/2})$. The plasmoid arrival at 0252 UT is preceded by 3.16 kHz electron plasma oscillations, right-hand magnetosonic waves, and an intense low frequency emission below 178 Hz. The plasma sheet contains broadband electrostatic noise which extends from 31 Hz to 5.6 kHz. After the slow shock of 0302 UT, the electron plasma frequency increased from 1.78 kHz to 5.6 kHz as the density rose to values typical of the magnetotail boundary layer. The intense emissions of 178 Hz and 316 Hz are characteristic of the tail boundary layer region.

Figure 2 - The plasma density, temperature, and flow speed measured by the LANL electron analyzer for the five events discussed in this paper.

Figure 3 - Selected electric field amplitude spectra for the frequency range 17.8 Hz to 100 kHz during the January 27, 1983, event. The lower curve is the average spectrum over a one minute interval which starts at the indicated time. The top curve is the spectrum formed from the peak amplitude which occurred in each frequency channel during the one minute interval.

Figure 4 - The magnetic field and plasma wave measurements for the plasmoid (0542 UT and 0617 UT) and slow shock (0552 UT) events on February 4, 1983. The strong 178 Hz and 316 Hz omissions from 0530 to 0538 UT and 0600 to 0612 UT are typical of the magnetotail boundary

layer. The impulsive waves from 56 Hz to 316 Hz which occur from 0550 UT to 0600 UT and after 0626 UT are the narrowband emissions characteristic of the region upstream of slow shocks.

Figure 5 - Selected electric field amplitude spectra for the February 4, 1983, events.

Figure 6 - The magnetic field and plasma wave measurements for the two plasma sheet encounters on February 7, 1983. The intense 316-562 Hz emissions near 1218 UT indicate that ISEE-3 was in the tail boundary layer just before entering the plasma sheet boundary layer at 1218 UT. In the interval 1216 UT to 1236 UT, the spacecraft remained in the outer layer or leading edge of the slow shock at the edge of the plasma sheet; the wave spectra represent a mixture of the peaked emissions detected upstream of slow shocks and the broadband noise observed in the downstream plasma sheet. From 1246 UT to 1255 UT, ISEE-3 reentered the tail boundary layer. The sharp onset of 5.6 kHz electron plasma oscillations of 1255 UT indicate that the satellite was once again on lobe field lines which connect to the plasma sheet.

Figure 7 - Selected electric field amplitude spectra for the February 7, 1983, events.

Figure 8 - Magnetic field and plasma wave measurements for the plasma sheet boundary layer encountered on February 10, 1983. From 0300 to 0310 UT, the wave emissions consisted of electron plasma oscillations at 5.62 kHz and low frequency noise with a broad spectral peak centered at 178 Hz. Strong plasma flow started at 0312 UT and continued until after 0400 UT. The plasma sheet boundary layer is characterized by strong field-aligned plasma flow, broadband electrostatic noise, and electron plasma oscillations. During the

interval 0322 UT to 0400 UT, the electron plasma frequency increased from 3.16 kHz to 10 kHz, which corresponds to the electron density rising from 0.1 cm^{-3} to 1.0 cm^{-3}. The LANL measured electron density in the energy range 10 ev to 1 keV remained constant at 0.1 cm^{-3}, indicating the presence of a moderately dense population of cold electrons.

Figure 9 - Selected electric field amplitude spectra for the event on February 10, 1983.

Figure 10a - Magnetic field and plasma wave measurements for the period 0800-0845 UT on March 25, 1983. At 0811 UT, the oncoming plasmoid (0824-0847 UT) was heralded by the arrival of >75 keV electrons and the sudden onset of very intense electron plasma oscillations at 5.6 kHz. The intense low frequency waves which began after 0813 UT consists of a mixture of electrostatic noise and narrowband whistler mode emissions. Broadband electrostatic noise and whistlers persisted within the plasmoid-plasma sheet region. Near 0875 UT, ISEE-3 encountered an unusual magnetic structure in which the plasma sheet field was directed predominately dawnward and northward. After leaving the plasma sheet at 0840, the strong low frequency emissions exhibit a spectral peak at 178 Hz that is similar to the frequency peak of the narrowband noise observed upstream of slow shocks in which the upstream magnetic field strength was smaller by a factor of two or more; thus, the peak frequency of these emissions is relatively insensitive to the magnetic field magnitude.

Figure 10b - Continuation of Figure 10a for the interval 0845-0930 UT on March 25, 1983. From 0845 to 0902 UT, the spectral peak of the low frequency emissions decreased from 316 Hz to 100 Hz. While the field

strength and plasma density remained constant, a very intense low frequency burst occurred at 0858 UT. The plasma sheet crossing is unusual in that the field strength remained above 10 nT; when $B_x = 0$, the field was directed dawnward. At 0920 UT, the onset of peaked 316 Hz waves indicate that ISEE-3 passed into magnetotail boundary layer.

Figure 11a - Selected electric (left) and magnetic (right) amplitude spectra for 0800-0845 UT on March 25, 1983.

Figure 11b - Selected electric field amplitude spectra for the period 0845 to 0930 UT on March 25, 1983.

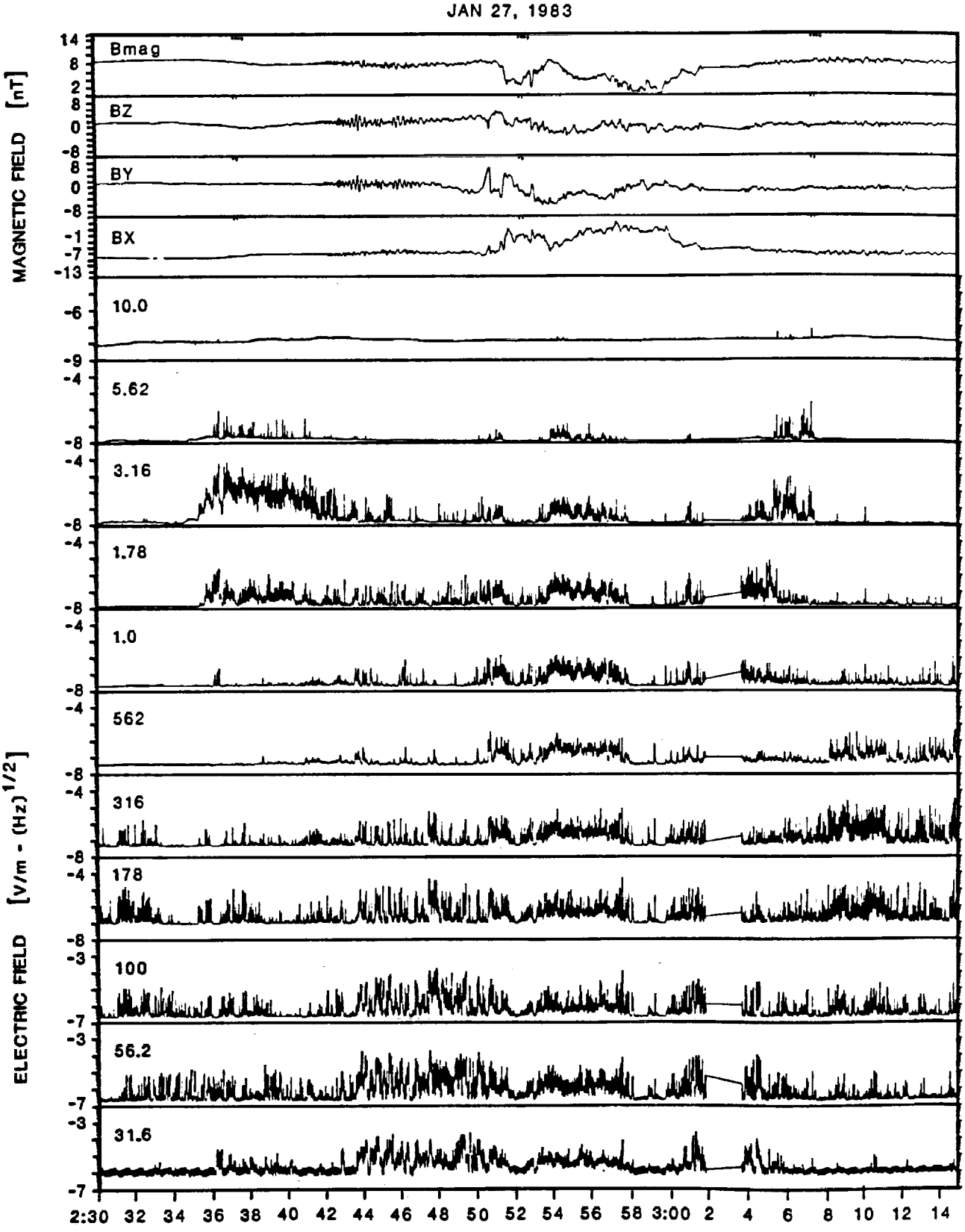
JAN 27, 1983
MAGNETIC FIELD [nT]
ELECTRIC FIELD [V/m - (Hz)^1/2]
Bmag
BZ
BY
BX
10.0
5.62
3.16
1.78
1.0
562
316
178
100
56.2
31.6
2:30 32 34 36 38 40 42 44 46 48 50 52 54 56 58 3:00 2 4 6 8 10 12 14
89-3

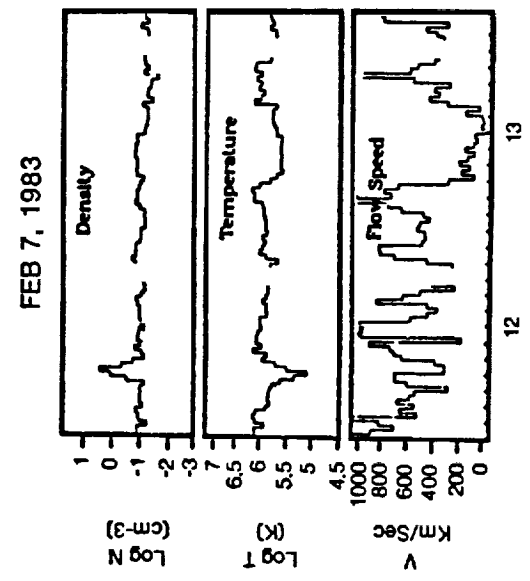
FEB 7, 1983
Density
Temperature
Flow Speed
Log N (cm-3)
Log T (K)
V Km/Sec
12
13

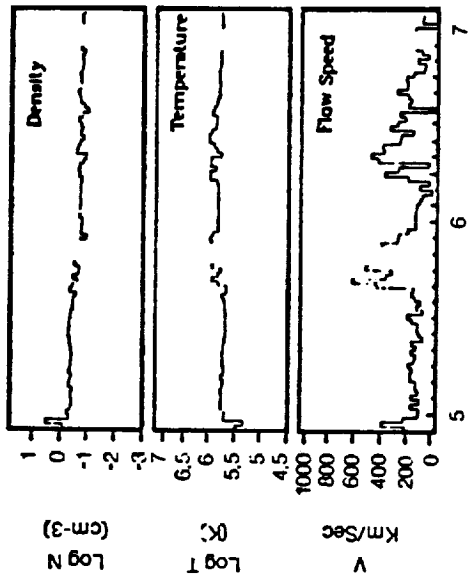
FEB 2, 1983
Density
Temperature
Flow Speed
Log N (cm-3)
Log T (K)
V Km/Sec
5
6
7

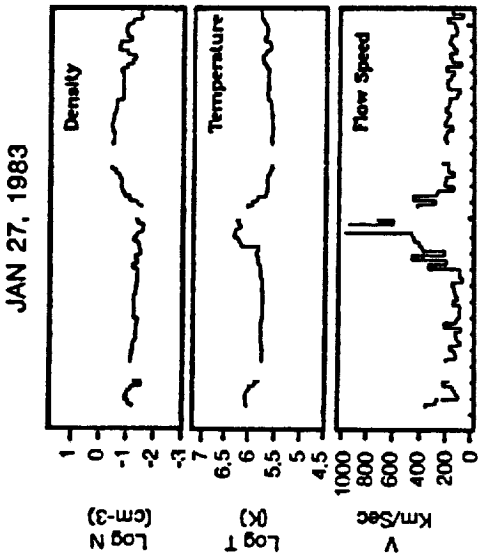
JAN 27, 1983
Density
Temperature
Flow Speed
Log N (cm-3)
Log T (K)
V Km/Sec
2
3
4

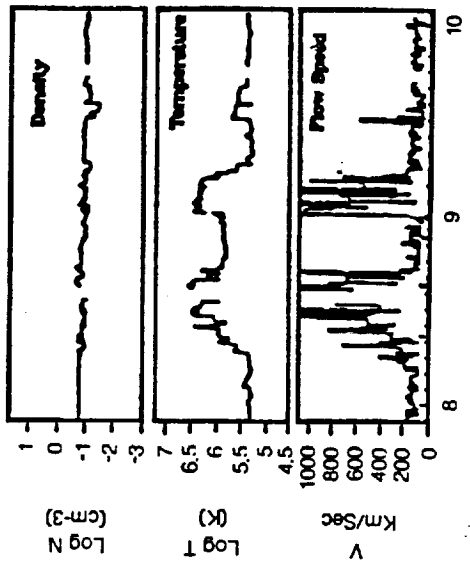
MAR 25, 1983
Density
Temperature
Flow Speed
Log N (cm-3)
Log T (K)
V Km/Sec
8
9
10

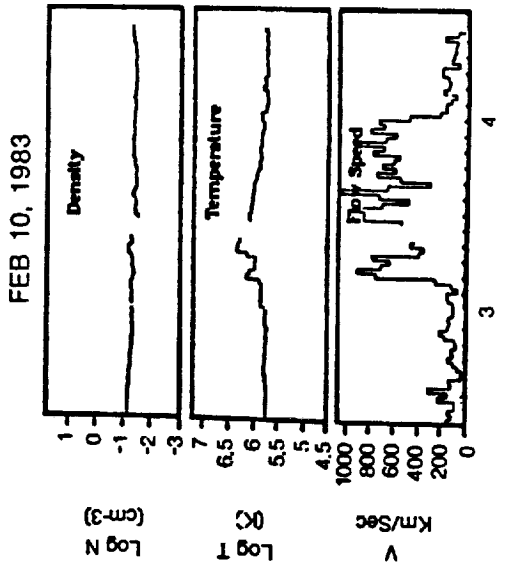
FEB 10, 1983
Density
Temperature
Flow Speed
Log N (cm-3)
Log T (K)
V Km/Sec
3
4

Fig. 2

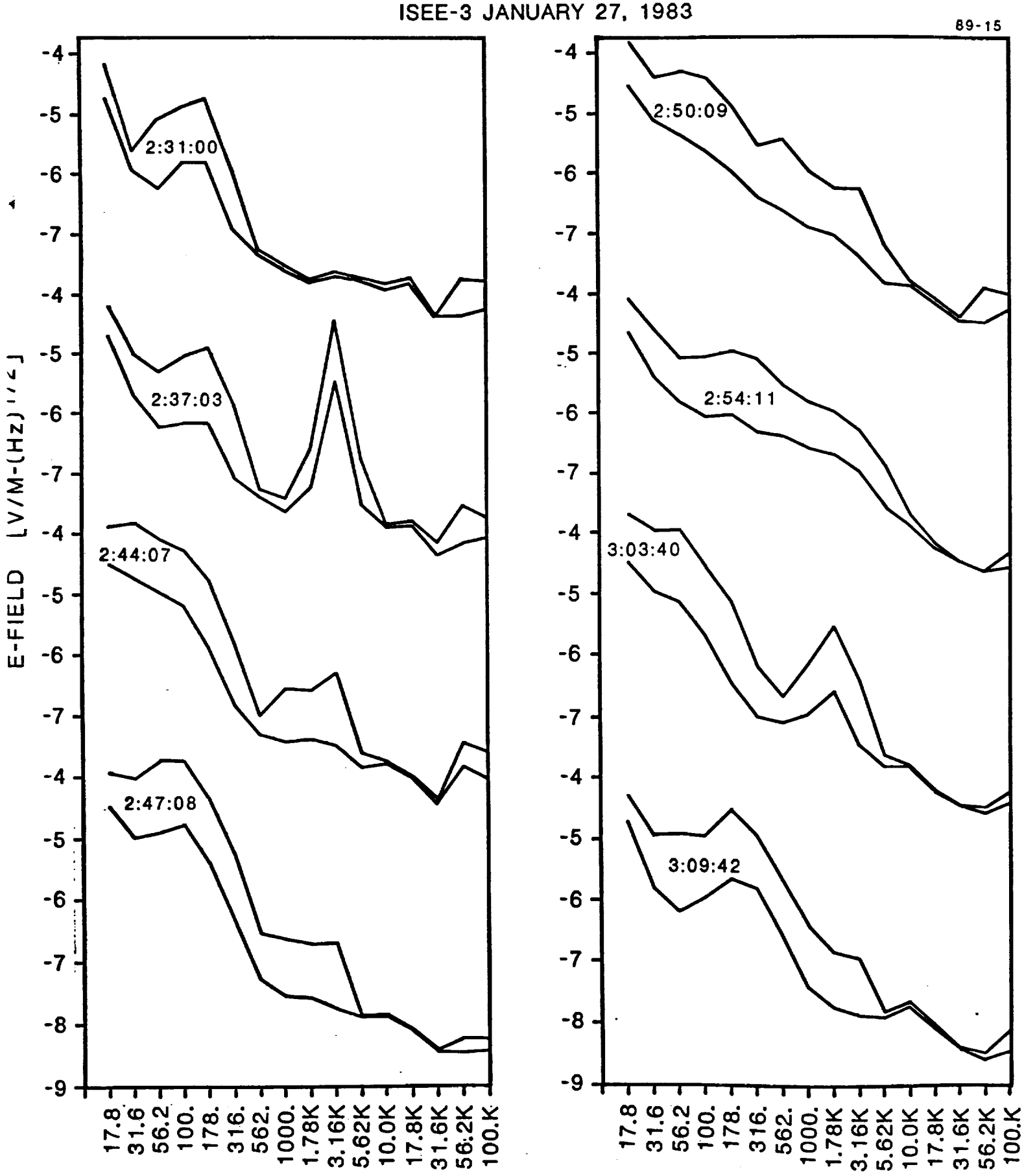
ISEE-3 JANUARY 27, 1983
89-15
E-FIELD [V/M-(Hz)^1/2]
2:31:00
2:37:03
2:44:07
2:47:08
2:50:09
2:54:11
3:03:40
3:09:42
-4
-5
-6
-7
-8
-9
17.8
31.6
56.2
100.
178.
316.
562.
1000.
1.78K
3.16K
5.62K
10.0K
17.8K
31.6K
56.2K
100.K

FEB 4, 1983

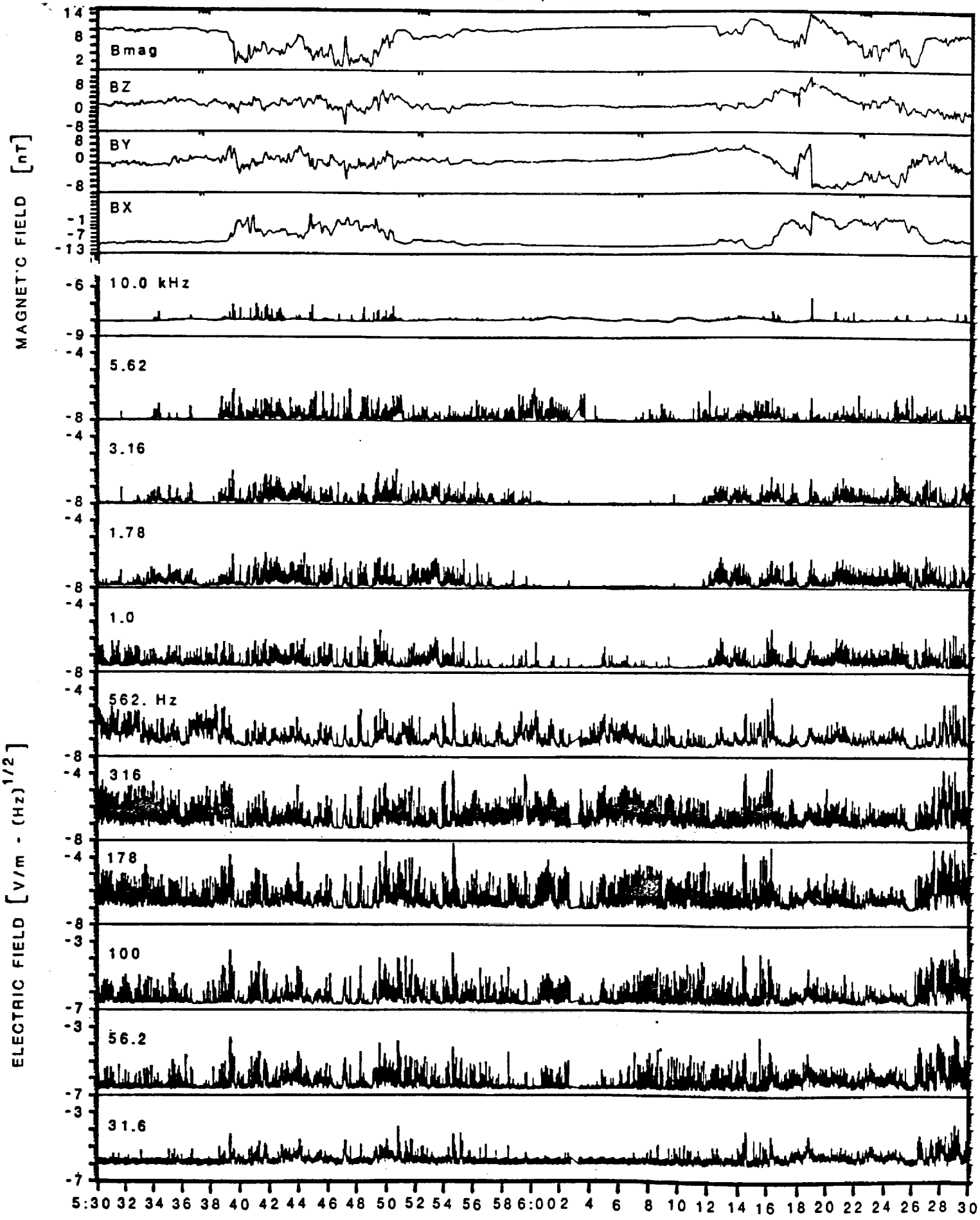
MAGNETIC FIELD [nT]
Bmag
BZ
BY
BX
10.0 kHz
5.62
3.16
1.78
1.0
562. Hz
316
178
100
56.2
31.6
ELECTRIC FIELD [V/m - (Hz)^1/2]
5:30 32 34 36 38 40 42 44 46 48 50 52 54 56 58 6:00 2 4 6 8 10 12 14 16 18 20 22 24 26 28 30

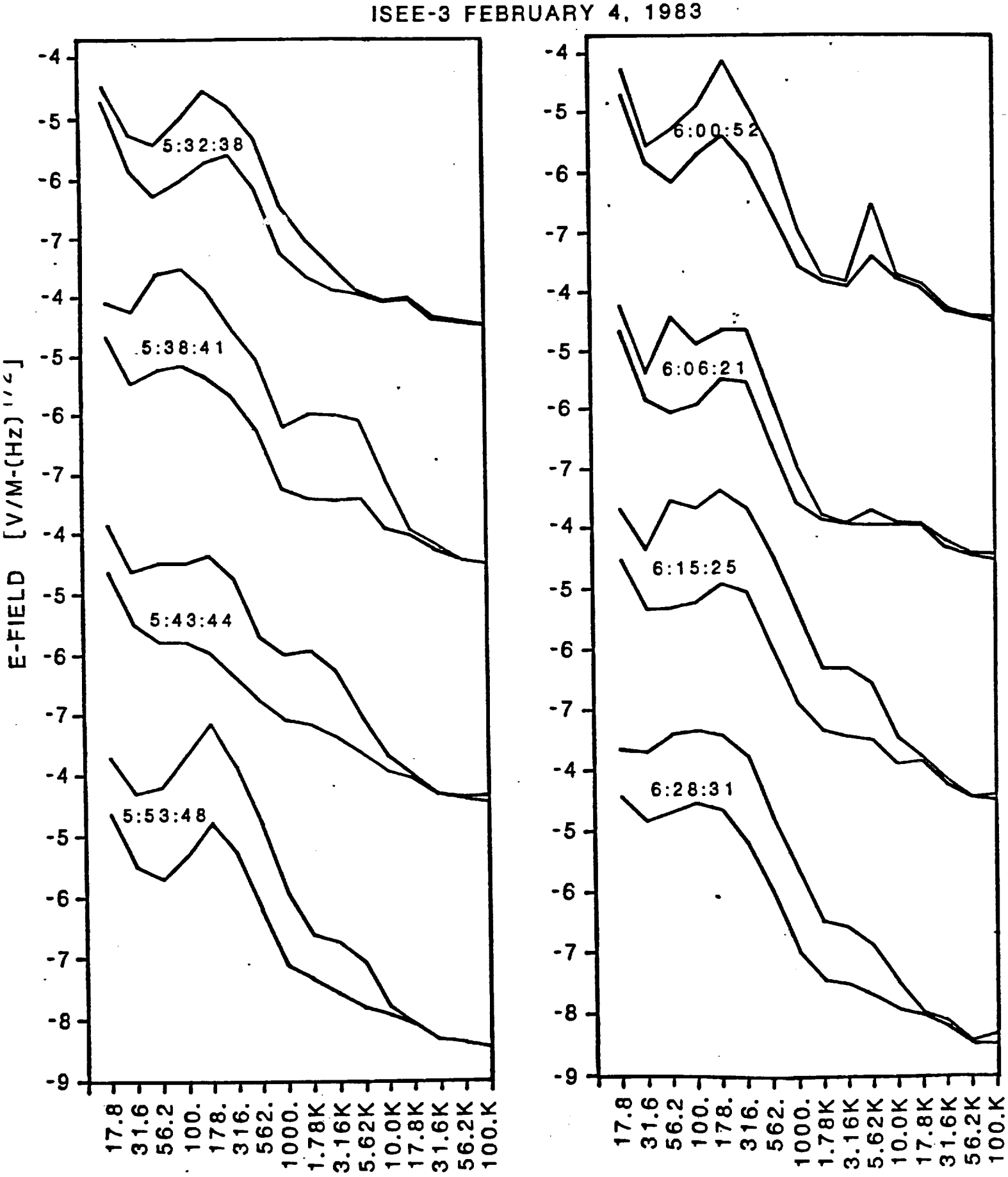
ISEE-3 FEBRUARY 4, 1983
E-FIELD [V/M-(Hz)^1/2]
5:32:38
5:38:41
5:43:44
5:53:48
6:00:52
6:06:21
6:15:25
6:28:31
-4
-5
-6
-7
-8
-9
17.8
31.6
56.2
100.
178.
316.
562.
1000.
1.78K
3.16K
5.62K
10.0K
17.8K
31.6K
56.2K
100.K

FEB 7, 1983

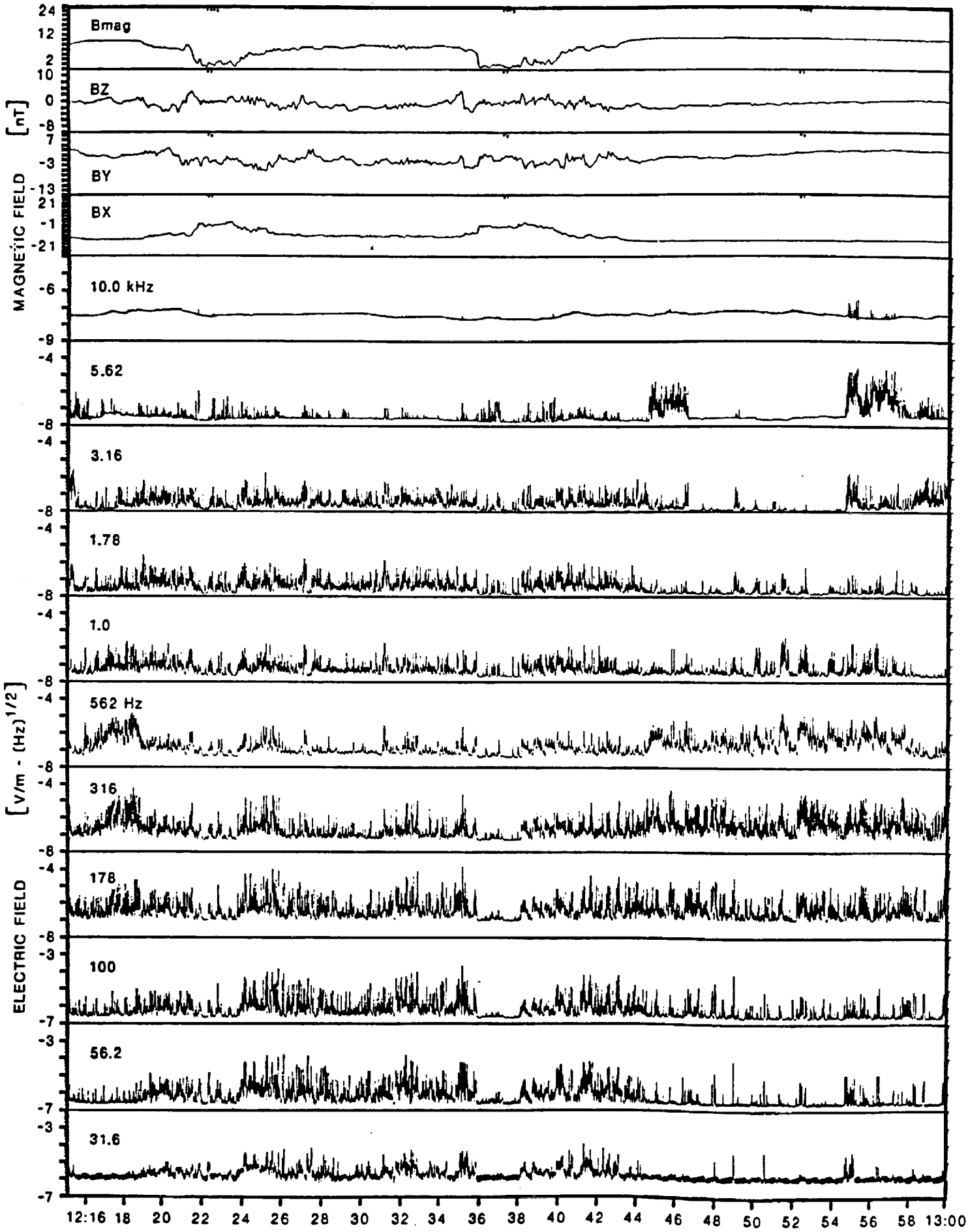
MAGNETIC FIELD [nT]
Bmag
BZ
BY
BX
ELECTRIC FIELD [V/m - (Hz)^1/2]
10.0 kHz
5.62
3.16
1.78
1.0
562 Hz
316
178
100
56.2
31.6
12:16 18 20 22 24 26 28 30 32 34 36 38 40 42 44 46 48 50 52 54 56 58 13:00

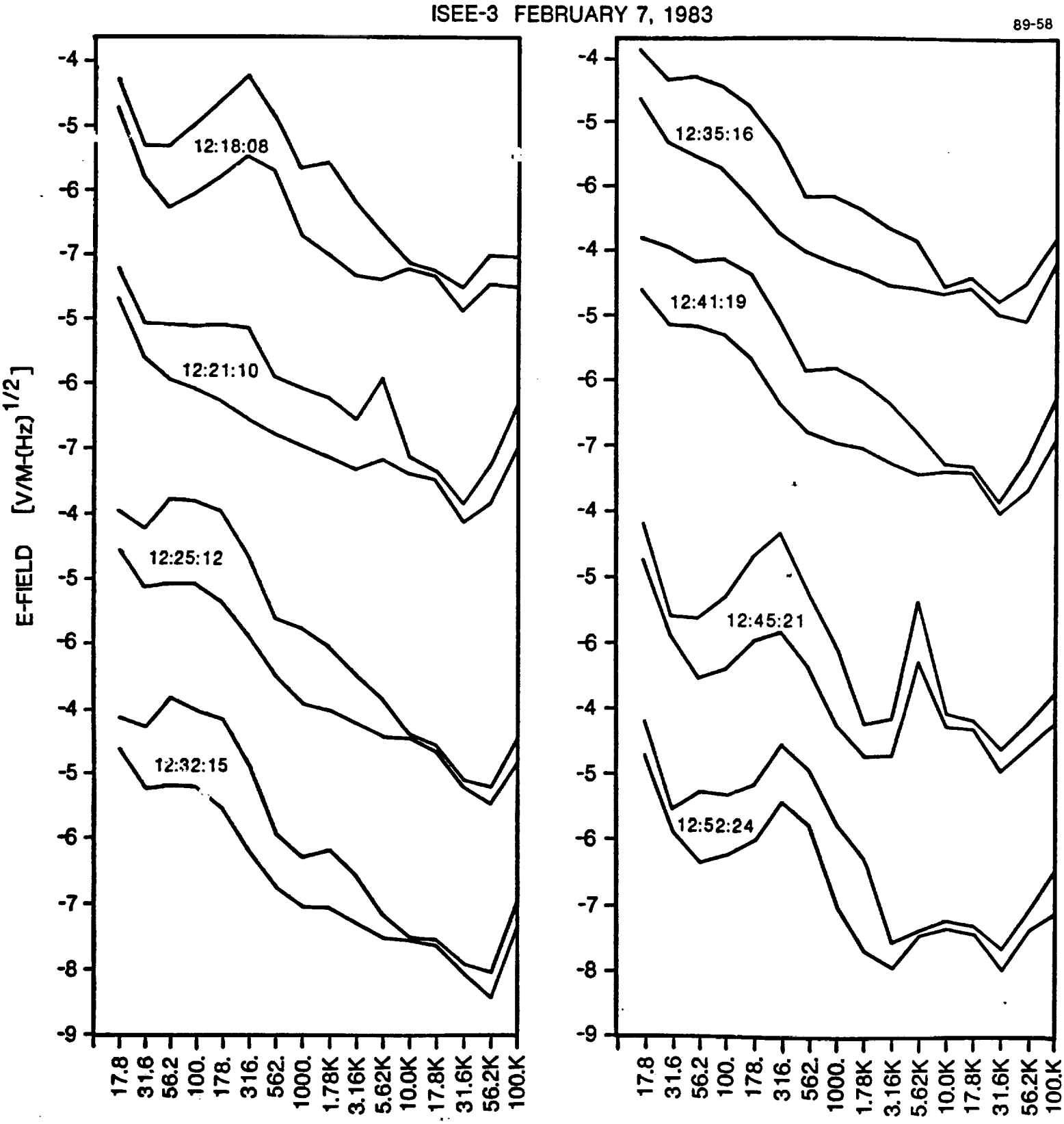
ISEE-3 FEBRUARY 7, 1983
89-58
E-FIELD [V/M-(Hz)$^{1/2}$]
12:18:08
12:21:10
12:25:12
12:32:15
12:35:16
12:41:19
12:45:21
12:52:24
-4
-5
-6
-7
-8
-9
17.8
31.6
56.2
100.
178.
316.
562.
1000.
1.78K
3.16K
5.62K
10.0K
17.8K
31.6K
56.2K
100.K

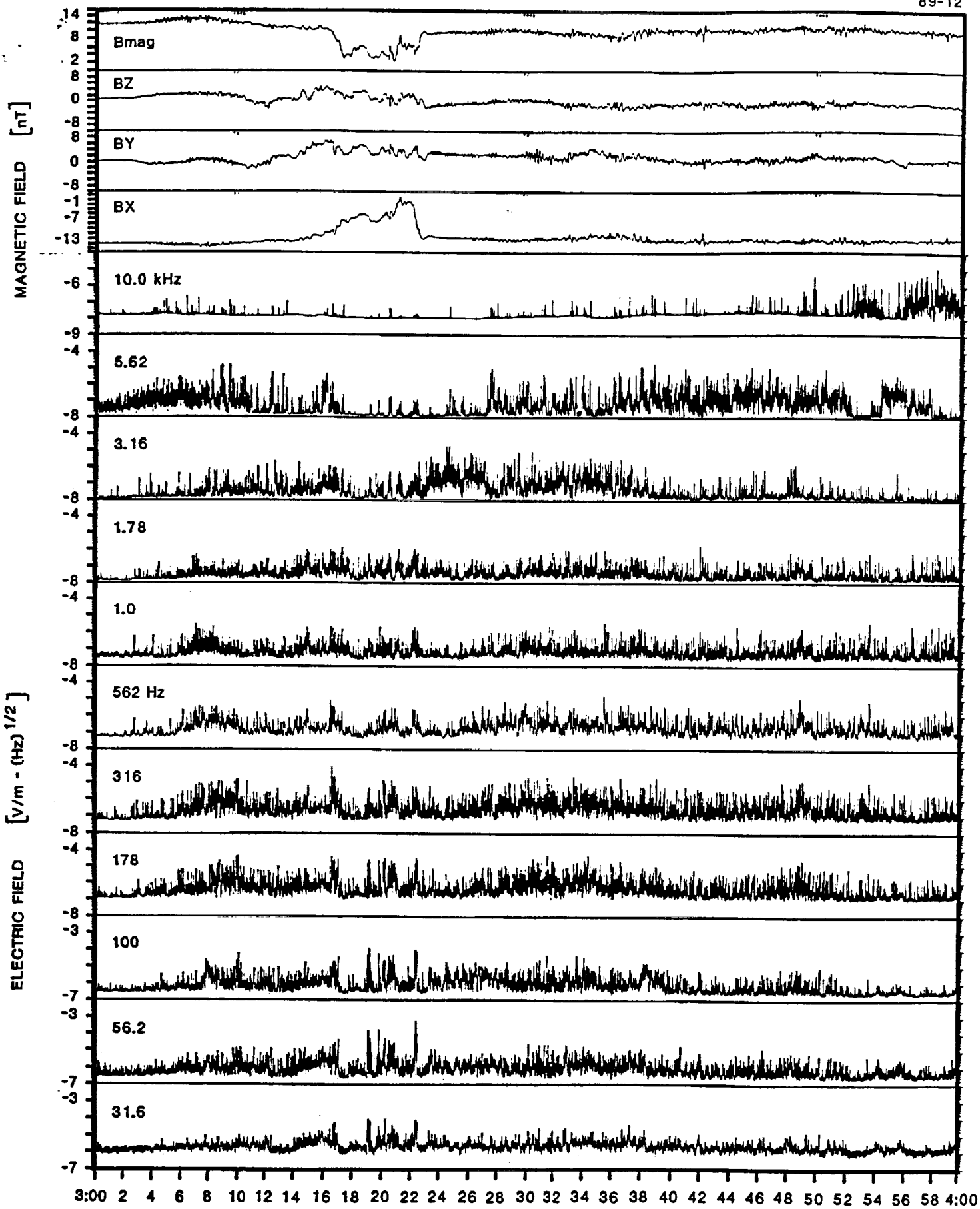
FEB 10, 1983
MAGNETIC FIELD [nT]
ELECTRIC FIELD [V/m - (Hz)^1/2]
Bmag
BZ
BY
BX
10.0 kHz
5.62
3.16
1.78
1.0
562 Hz
316
178
100
56.2
31.6
3:00 2 4 6 8 10 12 14 16 18 20 22 24 26 28 30 32 34 36 38 40 42 44 46 48 50 52 54 56 58 4:00

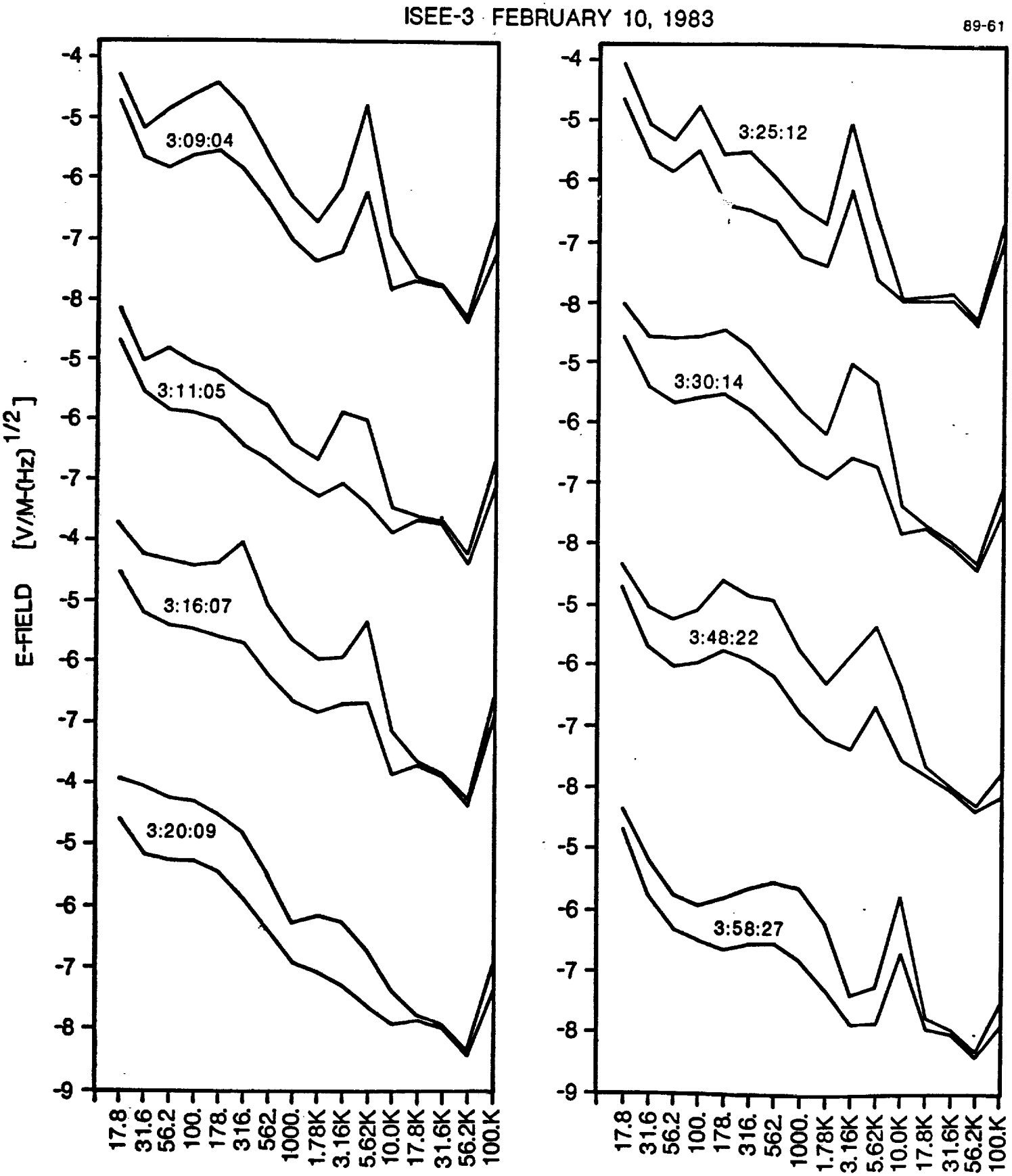
ISEE-3 FEBRUARY 10, 1983
89-61
E-FIELD [V/M-(Hz)^1/2]
3:09:04
3:11:05
3:16:07
3:20:09
3:25:12
3:30:14
3:48:22
3:58:27
-4
-5
-6
-7
-8
-9
17.8
31.6
56.2
100.
178.
316.
562
1000.
1.78K
3.16K
5.62K
10.0K
17.8K
31.6K
56.2K
100.K

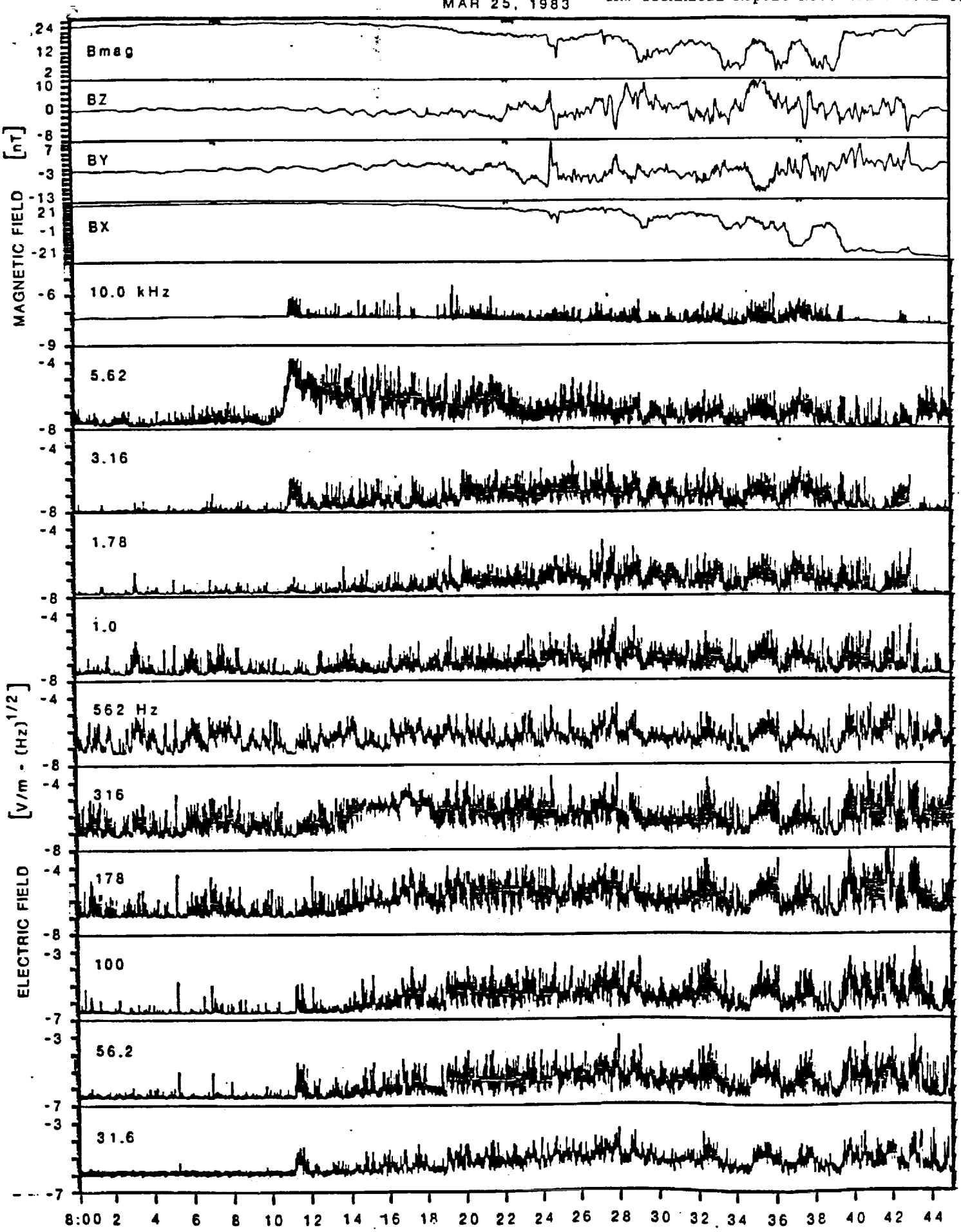
MAR 25, 1983
MAGNETIC FIELD [nT]
Bmag
BZ
BY
BX
ELECTRIC FIELD [V/m - (Hz)^1/2]
10.0 kHz
5.62
3.16
1.78
1.0
562 Hz
316
178
100
56.2
31.6
8:00 2 4 6 8 10 12 14 16 18 20 22 24 26 28 30 32 34 36 38 40 42 44

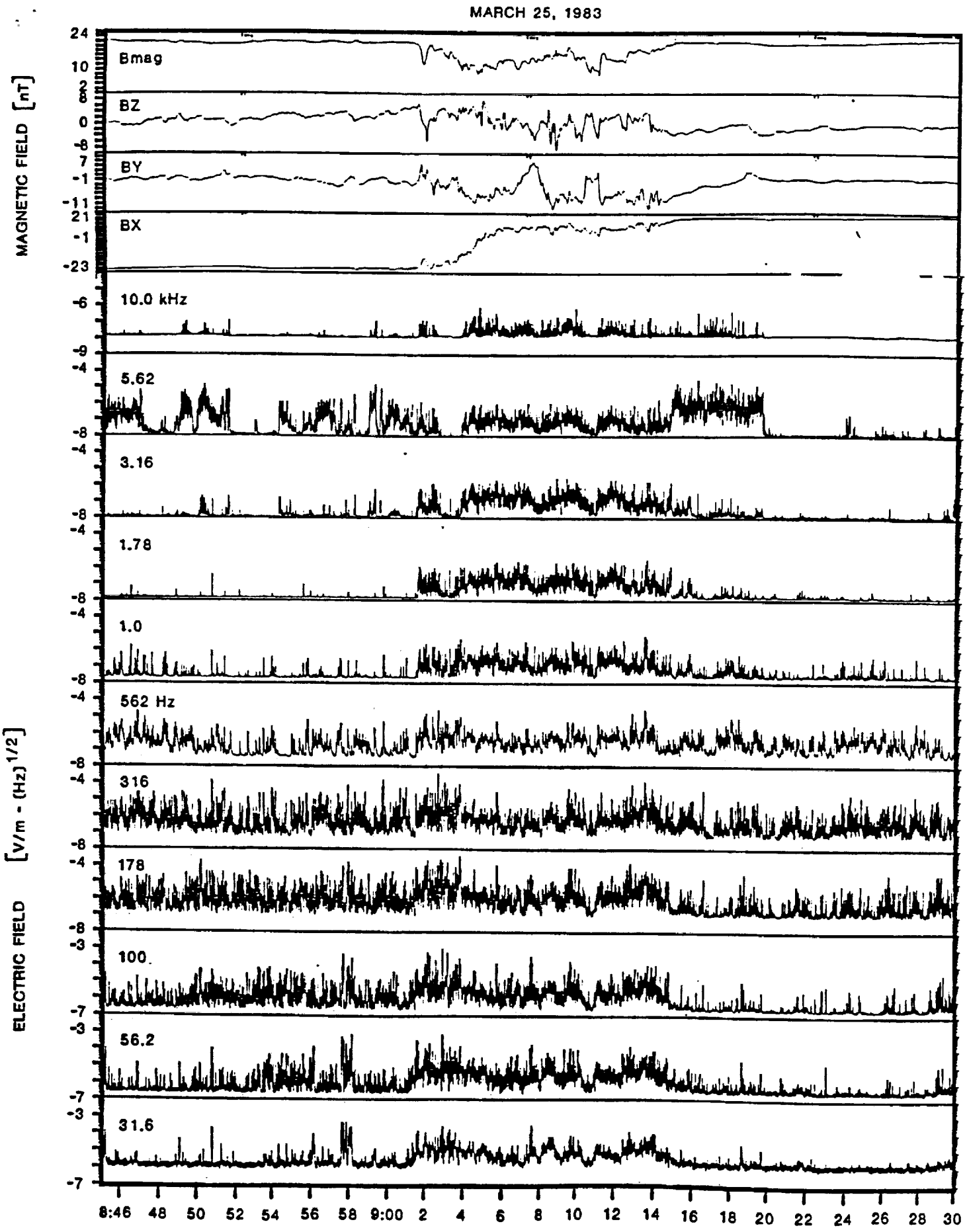
MARCH 25, 1983
MAGNETIC FIELD [nT]
Bmag
BZ
BY
BX
10.0 kHz
5.62
3.16
1.78
1.0
562 Hz
316
178
100
56.2
31.6
ELECTRIC FIELD [V/m - (Hz)1/2]
8:46 48 50 52 54 56 58 9:00 2 4 6 8 10 12 14 16 18 20 22 24 26 28 30

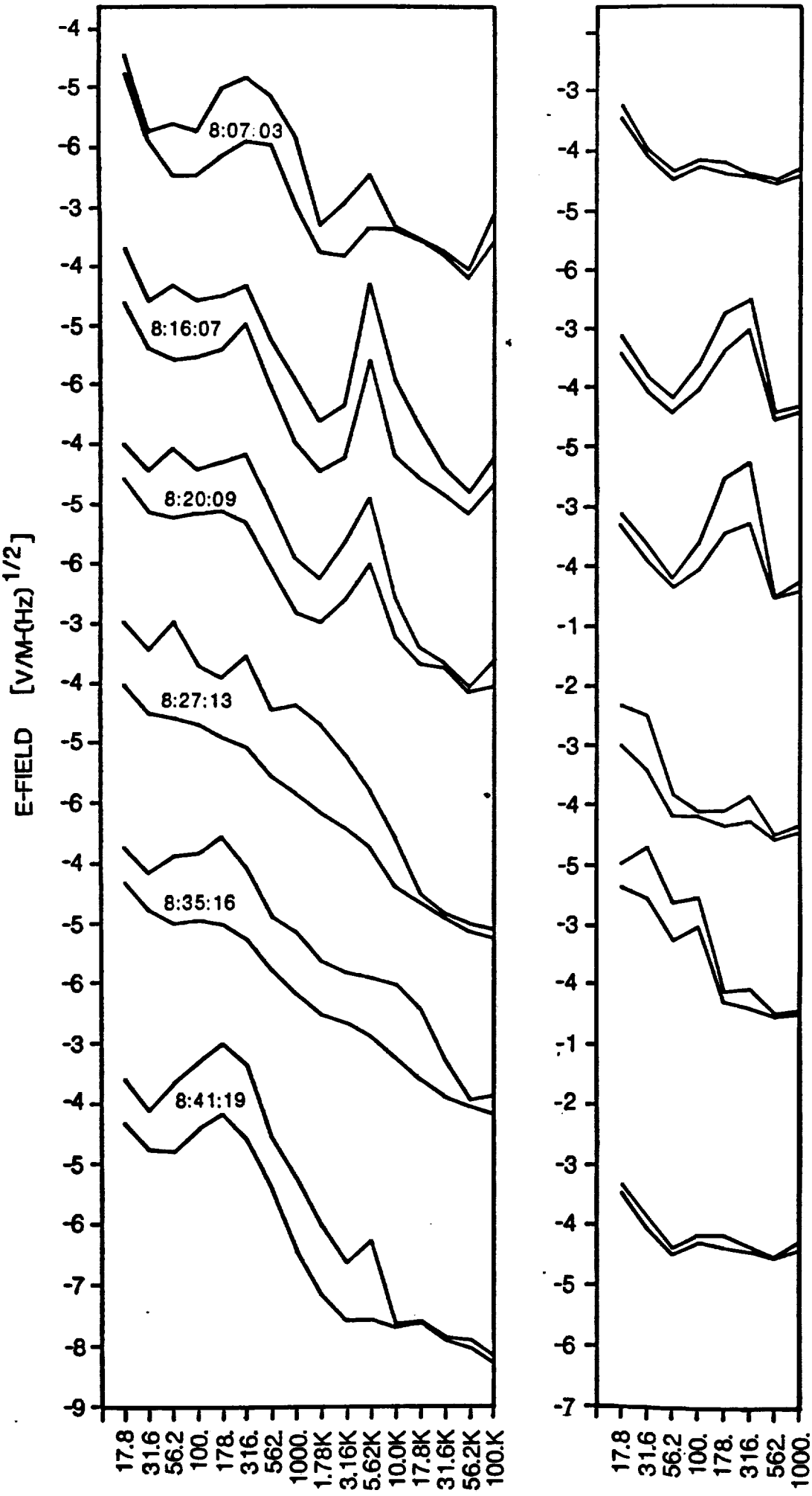
E-FIELD [V/M-(Hz)^1/2]
8:07:03
8:16:07
8:20:09
8:27:13
8:35:16
8:41:19
-4
-5
-6
-3
-4
-5
-6
-4
-5
-6
-3
-4
-5
-6
-3
-4
-5
-6
-4
-5
-6
-3
-4
-7
-8
-9
17.8
31.6
56.2
100.
178.
316.
562
1000.
1.78K
3.16K
5.62K
10.0K
17.8K
31.6K
56.2K
100.K
-3
-4
-5
-6
-4
-5
-6
-3
-4
-5
-6
-1
-2
-3
-4
-5
-6
-4
-5
-6
-1
-2
-3
-4
-5
-6
-7
17.8
31.6
56.2
100.
178.
316.
562
1000.

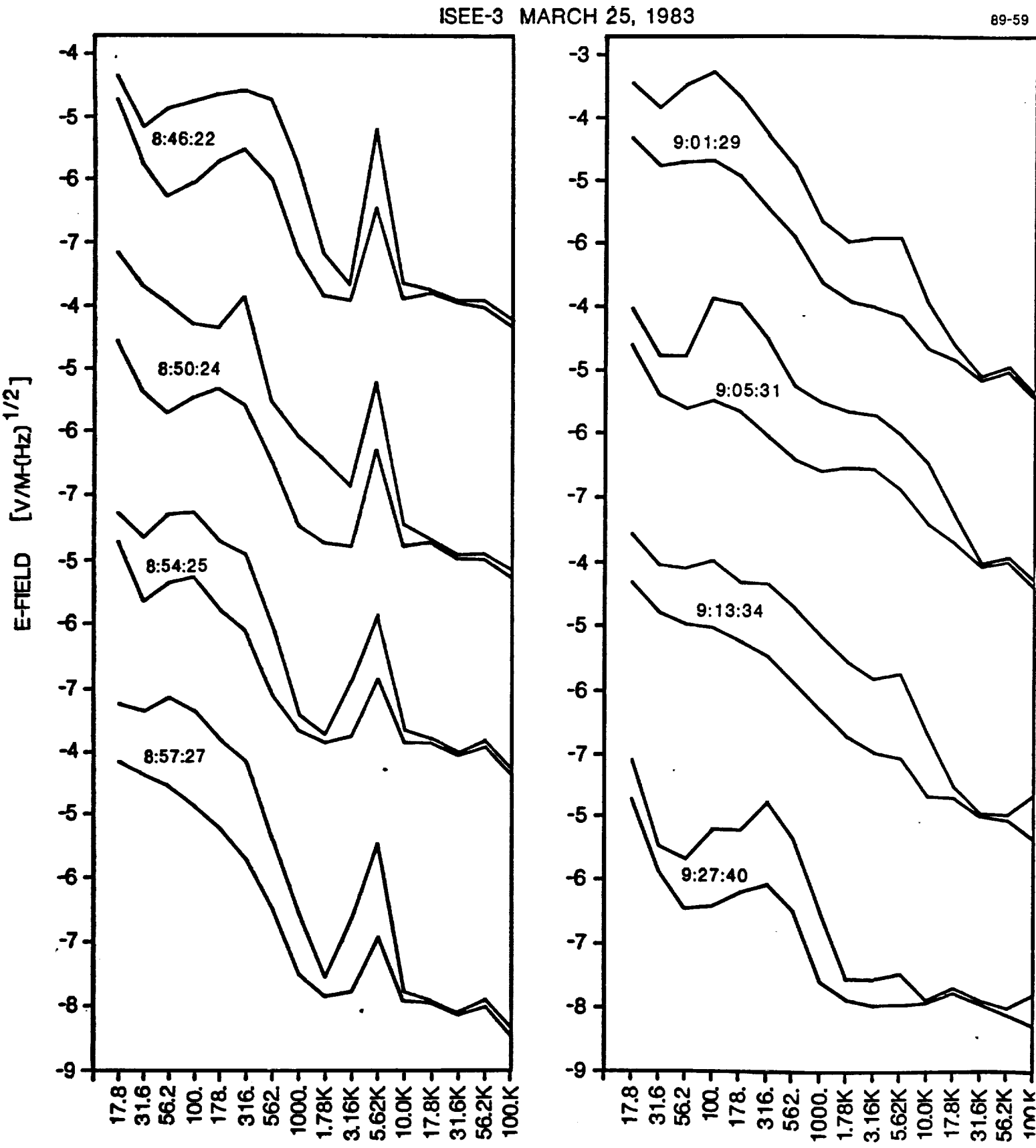
ISEE-3 MARCH 25, 1983
89-59
E-FIELD [V/M-(Hz)$^{1/2}$]
8:46:22
8:50:24
8:54:25
8:57:27
9:01:29
9:05:31
9:13:34
9:27:40
-4
-5
-6
-7
-8
-9
-3
17.8
31.6
56.2
100.
178.
316.
562.
1000.
1.78K
3.16K
5.62K
10.0K
17.8K
31.6K
56.2K
100.K

APPENDIX B

Greenstadt et al., DRAFT Report

APPENDIX B

Greenstadt et al., DRAFT Report

Observations of the Flank of Earth's Bow Shock to −110 R_E by ISEE-3/ICE

E. W. Greenstadt, D. P. Traver, and F. V. Coroniti

Physical Sciences Department, TRW

E. J. Smith

Jet Propulsion Laboratory

J. A. Slavin

NASA Goddard Space Flight Center

Abstract. Among the invaluable and unique sets of observations made by the ISEE-3/ICE spacecraft during the lunar and multiple Earth swingbys that set its course for comet Giacobini-Zinner, there were well over 100 crossings of Earth's bow shock between X(SEC)= −20 and −110 R_E, most of them further away than −60 R_E. Mach numbers normal to the shock in this extreme downwind flank of the bow shock are generally no more than about 60% of their unprojected values in the solar wind, so that this set of crossings consists of many more examples of low magnetosonic M_{MS} ($M_{MS}<3$) crossings than have been acquired in the subsolar region, including rare quasi-parallel, as well as quasi-perpendicular, cases. We tabulate the parameters of the crossings, display some of their magnetic, plasma wave, and spectral profiles at low M, and compare loci of crossings with an extrapolation of the most statistically complete model of the shock to date, showing that the model remains useful in the far flank.

INTRODUCTION

Two fundamental questions, one global and macroscopic, the other local and microscopic, still remain open about the distant Earth's bow shock far downstream behind the geomagnetosphere: First, how well do models of the shock's shape extrapolate to great distances where the shock approaches its theoretical fluid Mach cone? Second, does the expected reduction of local Mach numbers by the extreme attack angle of the distant shock offer a useful view of very low Mach number, i.e., subcritical, shock

structures? To date, relatively few low Mach number shocks, especially subcritical, quasi-parallel ones have been documented [*Mellott*, 1985 (review and references therein); *Mellott and Greenstadt*, 1987; *Greenstadt and Mellott*, 1988]. More examples would be helpful if they were to offer new or rare conditions.

Fortunately, these questions need no longer be posed as abstract exercises. During its prolonged, 14 month sojourn around the earth in preparation for its diversion to comet Giacobini-Zinner, ISEE-3 passed many (>100) times through the distant shock. Most of its shock observations were obtained at greater distances than had been sampled before, providing a rich source of low Mach number cases. This report offers affirmative answers to the questions posed above and a preliminary look at some shock examples.

Although a number of studies of the distant, or "deep" geomagnetic tail with ISEE-3 data have been published (e.g. *Feldman, et al., 1984; Richardson and Cowley, 1985; Scarf et al.,1984*), the reader may not readily associate the familiar ISEE-3 or ICE missions with the relatively unfocused and unfamiliar operations of the spacecraft during the complicated swings around the Earth-Moon system that took the spacecraft also into the foreshock, shock, and magnetosheath. The originally designated ISEE-3, launched in 1978, had as its mission the observation of the solar wind around the Lagrangian point some 200 R_E sunward from Earth. After its final lunar assist and redirection to G-Z in December 1983, it was renamed ICE, for "International Cometary Explorer."

Strictly speaking, the portion of the redirected mission spent around the earth was neither that intended for ISEE-3 nor for the subsequently renamed ICE, and represents a separate operation inappropriately designated by the names associated with either of the two other well known missions or by the awkward composite ISEE-3/ICE. Because of the unique, distinct, and, we believe, important mission defined by its status as an earth satellite predominantly downwind from Earth, and for need of a quickly identifiable name for the segment of the mission we are investigating, we shall refer to the satellite in this paper as IDE, for "International Downwind Explorer." In the following sections we summarize the global perspective in which the IDE observations were made, show some examples of flank shock profiles, and discuss the significance of this preliminary survey. We draw on data from the ISEE-3 magnetometer [*Frandsen et al.*, 1978] and plasma wave detector [*Scarf et al.* 1978], and we freely use the abbreviations q- in place of quasi- in the terms quasi-perpendicular and quasi-parallel.

GLOBAL CONTEXT OF THE IDE CONTRIBUTION

Shock model. Figure 1 is a three-dimensional computer sketch of the bow shock in the SEC coordinate system centered at Earth, superposed on a composite scatter plot of all the shock crossings to which the most comprehensive and most recent shock model was fit by Slavin *et al.* [1984]. The shock is represented by its Y=0, Z=0, X=0, and X=-20 cross sections. The average hyperboloid of revolution matched to the data by Slavin *et al.*, is given in rectangular coordinates by

$$\rho^2 = Y^2 + Z^2 = A[(X - B)^2 + C], \qquad (1)$$

where A=.04, B=566.4, and C=304,682.

When introduced, the model represented an advance over previous models because it included crossings on the flank of the shock behind the earth not available to earlier surveys. Note, however, that few of the "flank" observations had then occurred further behind the X=0 plane than X=-20, and that the bulk of the X<0 data came from high northern latitudes. Whether the model fit to these data might represent the shock at more extreme positions along its flanks and at low latitudes remained an open question.

The data set. The locations of all the identified crossings of the bow shock by ISEE-3 for X<-20 are collected in Figure 2. Each numbered trajectory segment is the X-Y projection of the satellite's path from the first to the last of a series of shock crossings. All the IDE's maneuvers in the earth's downwind and tail region took place close to the ecliptic plane so that the neglected Z-coordinate in the trajectory projections of the figure are relatively insignificant. At the distances of the observations, the Z-position of the spacecraft was never more than 22.5 R_E, usually less than 8 R_E from the X-Y plane on the flank; hence, the Y-coordinate was never less than 95%, usually more than 98%, of the cylindrical coordinate ρ. At X=-60R_E, the difference between the projected Y' of the spacecraft and the ρ of the model was less than 2-3 thicknesses of the lines in the figure.

The bow shock cross section in Figure 2 is the average model shock given by equation (1), plotted with ρ=Y and tilted slightly clockwise by 4° to account for the solar wind abberation that appeared to provide the best visual fit of the shock crossings taken as a group. We see that the 4° rotation put the predawn flank of the shock close to the middle of all the trajectory segments on that side. We have no information yet with which to decide whether segment 1's location entirely inside the shock on the opposite side was caused by unusual solar wind or asymmetry unaccounted for in the shock model. We ignore segments 4 and 6 in this study.

Projected Mach number. The local Mach numbers of IDE's shock crossings are significantly reduced from their free-stream, or subsolar, values when the component of solar wind velocity projected on the local normal is taken into account. Figure 3 contains plots of both θ_{Xn} and cos (θ_{Xn}) *vs* X for the shock model of this report. The upper graph shows the large angle through which the solar wind velocity, assumed to be directed along -X, must be projected to obtain the Mach number applicable to the shock propagating along its local normal in the far flank; the lower graph shows the actual factor by which the free-stream Mach number is thereby reduced. At X -100 R_E, where several trajectory segments containing many shock crossings occurred (Figure 2), the outcome is to provide a considerable inventory of shock observations with Mach numbers only a third (cos 70°= .342) of their free stream values. The X-coordinates of segment 8 of Figure 2 are indicated between the graphs to emphasize this

point. Many, if not most, of these distant crossings must have had M<3, and most, if not all, must have been subcritical by theoretical definition [Edmiston and Kennel, 1984], since magnetosonic Mach numbers of the solar wind were generally between 4 and 7.

Histograms of the local Mach numbers of all IDE crossings, before and after reduction computed from the lower curve plotted in Figure 3, are shown in Figure 4. The effect on the Mach numbers of IDE's downwind position is dramatic. Most of the observed shock encounters were in a range of local Mach numbers below 2.5, previously recorded in only a handful of cases. Especially important is the large proportion, 41%, of quasi-parallel crossings whose reduced Mach numbers place them in a category of shock parameter space hitherto almost void of cases.

EXAMPLES

Figure 5 presents five of IDE's shock profiles. The top panel offers, for comparison with those below, a supercritical profile from the IDE data set, showing the typical sharp step and overshoot associated with Earth's bow shock, even for crossings only mildly in the range of quasi-perpendicular geometry (θ_{Bn}=58°) and only mildly "supercritical". The remaining, low Mach, cases progress toward the bottom panel from quasi-perpendicular to quasi-parallel according to θ_{Bn} computed from the model shock. The principal parameters for each case, β, M_{MS}, and θ_{Bn} are noted in each panel. The upper of the bracketed Mach numbers, M_θ, in each example is the reduced value computed by applying the appropriate geometrical factor to the corresponding free-stream Mach

number; the lower number, M_B, is the ratio of downstream to upstream field magnitude, which should approximate the Mach number defined by the shock profile itself. Occasionally, as in the second case from the bottom, the two Mach numbers essentially coincide; usually they differ by a few tenths. Uncertainties affecting these estimates are dominated, for M_Θ, by ignorance of the local shock speed and, for M_B, by difficulty in deciding exactly what "upstream" and "downstream" values to use except in the quietest cases.

The progression toward lower Θ_{Bn} shown in the figure is not "pure" in that the other parameters β and M are fixed only for the first two examples, but the profiles show the increasing contribution of waves, from two cycles of classical standing whistlers outside a smooth ramp when Θ_{Bn}=78° (1335, 31 Oct. 1982) to mixed frequencies of large relative amplitudes both up and downstream from the irregular ramp when Θ_{Bn}= 12° (0410, 23 Dec. 1983).

In Figure 6, we add one magnetic and two electric wave channels to the magnetometer plot of a shock crossing of very low Mach number and intermediate angle near the transition between q-perpendicular and q-parallel structures. We see that the shock exhibits clear plasma wave signatures, including a whistler "foot" similar to those associated with undetected reflected ions and undistinguishable magnetic feet in earlier studies [*Greenstadt and Mellott*, 1987; *Mellott and Greenstadt*, 1988]. The crossing of this example represents a profile as close to the

threshold of existence of a quasi-perpendicular shock as is likely to be found in satellite data, yet there is no difficulty in recognizing the event. The generalizability of the plasma wave foot phenomenon to all θ_{Bn}'s is one issue worthy of investigation.

DISCUSSION

The geometrically determined low Mach crossings on the far flank occurred in relatively stable locations where the shock would be expected simply by extrapolating to the large downwind distances of IDE a gasdynamic model based on observations much nearer the Earth. We therefore conclude that the extrapolated model is suitable to first order for representing the extended shock in general and, in particular, for estimating parameters needed for further study of the large population of low Mach number shock crossings provided by the 1982-83 maneuvers of ISEE-3 in and around the distant geomagnetic tail. Further, as the asymptotic Mach cone is approached, we do not find a significant "flapping" of the distant flank shock, but rather a steady shock phenomenon with well defined magnetic and plasma wave profiles even for very low Mach numbers or very low θ_{Bn}'s. In contrast, we have become accustomed, when attempting to study low Mach shock crossings into the subsolar region of Earth's shock, to exaggerated shock movement and standoff distances at higher than average local shock speeds. This unsteadiness in shock location seems to be a characteristic of the bow shock under the solar wind conditions associated with low free-stream Mach number and not with low local Mach number itself.

The IDE shock population represents the largest collection, by an order of magnitude, of low Mach number shocks ever found in space, and offers the opportunity to separate sets of cases that keep two of the principal shock parameters fixed while varying the third. Of particular interest is the large proportion of quasi-parallel crossings in the IDE set, a happy circumstance caused by the preferentially predawn trajectory of the satellite in the region where the average IMF favors q-parallel structure. Low Mach, q-parallel shocks are almost nonexistent in spacecraft data sets, and no example of a quasi-parallel, quasi-turbulent (low M, high β) shock has ever been published. We emphasize that the 100 or so count of shock crossings we have cited is biased toward q-perpendicular cases clearly identifiable in the magnetometer data alone. We believe that a significant augmentation of the q-parallel subset, and a few examples of quasi-turbulent profiles, will be obtained when plasma data are consulted as well. This collection justifies close scrutiny by all interested groups.

REFERENCES

Edmiston, J. P., and C. F. Kennel, A parametric survey of the first critical Mach number for a fast MHD shock, *J. Plasma Phys., 32,* 429-441, 1984.

Feldman, W. C., S. J. Schwartz, S. J. Bame, D. N. Baker, J. Bern, J. T. Gosling, E. W. Hones, Jr., D. J. McComas, J. A. Slavin, E. J. Smith, and R. D. Zwickl, Evidence for slow-mode shocks in the deep geomagnetic tail, *Geophys. Res. Lett., 11,* 599, 1984.

Frandsen, A. M. A., B. V. Conner, J. van Amersfoort, and E. J. Smith, The ISEE-C vector helium magnetometer, *IEEE Trans. Geosci. Elect., GE-16,* 195-198, 1978.

Greenstadt, E. W., and M. M. Mellott, Plasma wave evidence for reflected ions in front of subcritical shocks: ISEE 1 and 2 observations, *J. Geophys. Res., 92,* 4730-4734, 1987.

Mellott, M., M., Subcritical collisionless shock waves, in *Collisionless Shock Waves in the Heliosphere: Reviews of Current Research,* B. Tsurutani and R. Stone, eds., Am. Geophys. Union, Geophysical Monograph Series Vol. 35, 1985.

Mellott, M. M., and Greenstadt, E. W., Plasma waves in the range of the lower hybrid frequency: ISEE 1 and 2 observations at the earth's bow shock, *J. Geophys. Res., 93,* 9695-9708, 1988.

Richardson, I. G., and S. W. H. Cowley, Plasmoid-associated energetic ion bursts in the deep geomagnetic tail: Properties of the boundary layer, *J. Geophys. Res., 90,* 12,133, 1985.

Scarf F. L., f. V. Coroniti, C. F. Kennel, R. W. Fredricks, D. A. Gurnett, and E. J. Smith, ISEE-3 wave measurements in the distant geomagnetic tail and boundary layer, *Geophys. Res. Lett., 11,* 335, 1984.

Scarf, F. L., R. W. Fredricks, D. A. Gurnett, and E. J. Smith, The ISEE-C plasma wave instrument, *IEEE Trans. Geosci. Elect., GE-16,* 191-195, 1978.

Slavin, J. A. R. E. Holzer, J. R. Spreiter, and S. S. Stahara, Planetary Mach cones: Theory and observation, *J. Geophys. Res., 89,* 2708, 1984.

FIGURE CAPTIONS

Fig. 1. Composite three-dimensional scatter diagram of crossings of Earth's bow shock by several satellites, with superimposed computer sketch of cross sections of the best fit model used in this report. All but a few scattered crossings were obtained sunward of the shock's $X=-20R_E$ cross section (large oblique circle).

Fig. 2. Segments of the IDE trajectory that included bow shock crossings. The crossings were spaced at varying distances along the flank of the shock, straddling an extrapolation of model with 4° abberation.

Fig. 3. Upper panel: the angle θ_{Xn} of the local normal to the solar wind; lower panel: the factor cos θ_{Xn} by which the free stream Mach number is reduced to estimate the local Mach number of each crossing. Both quantities are calculated from the slope of the model hyperboloid of revolution.

Fig. 4. Distributions of free stream Mach numbers for the collected crossings (dashed histogram), local Mach numbers of the observed shock encounters determined from the model geometrical factor cos θ_{Xn} (solid histogram), and local Mach numbers of just the quasi-parallel crossings (shaded histogram).

Fig. 5. A selection of shock magnetic profiles showing progressive change from quasi-perpendicular to quasi-parallel structure.

Fig. 6. Plasma wave and magnetic field profile of a very weak transitional shock.

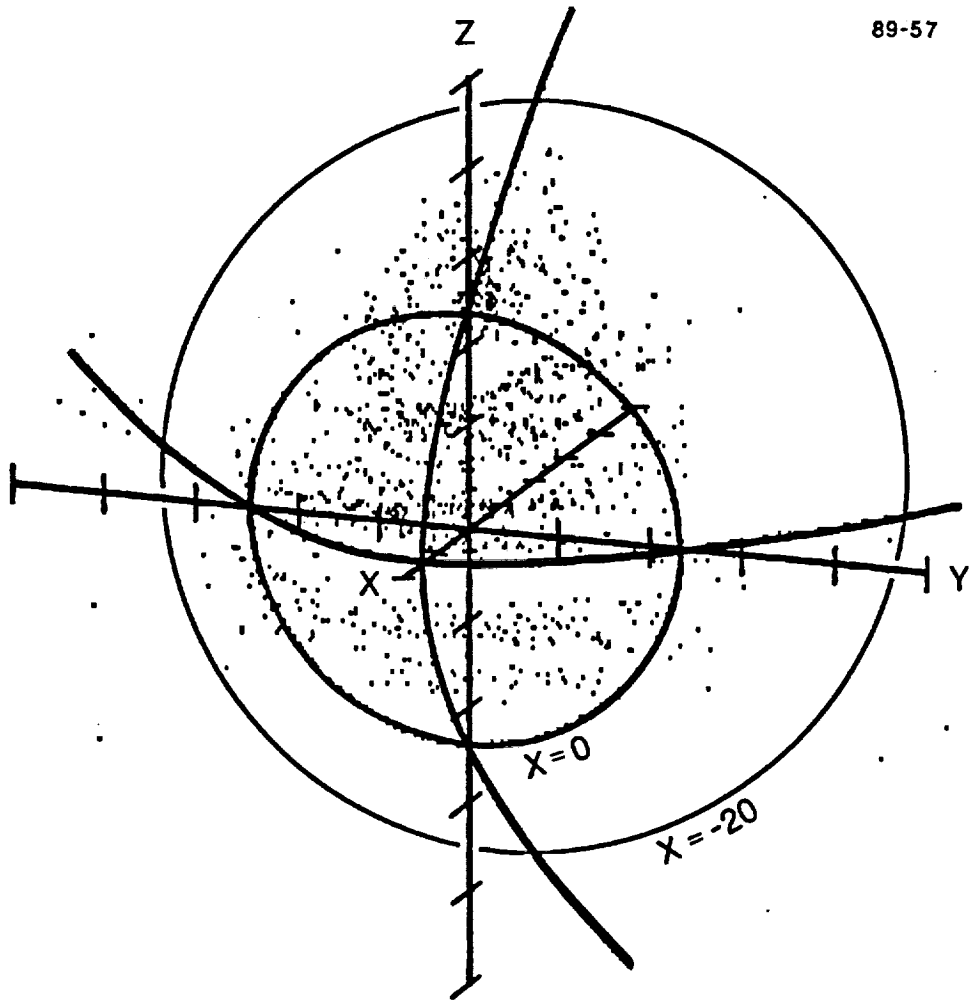

FIG. 1

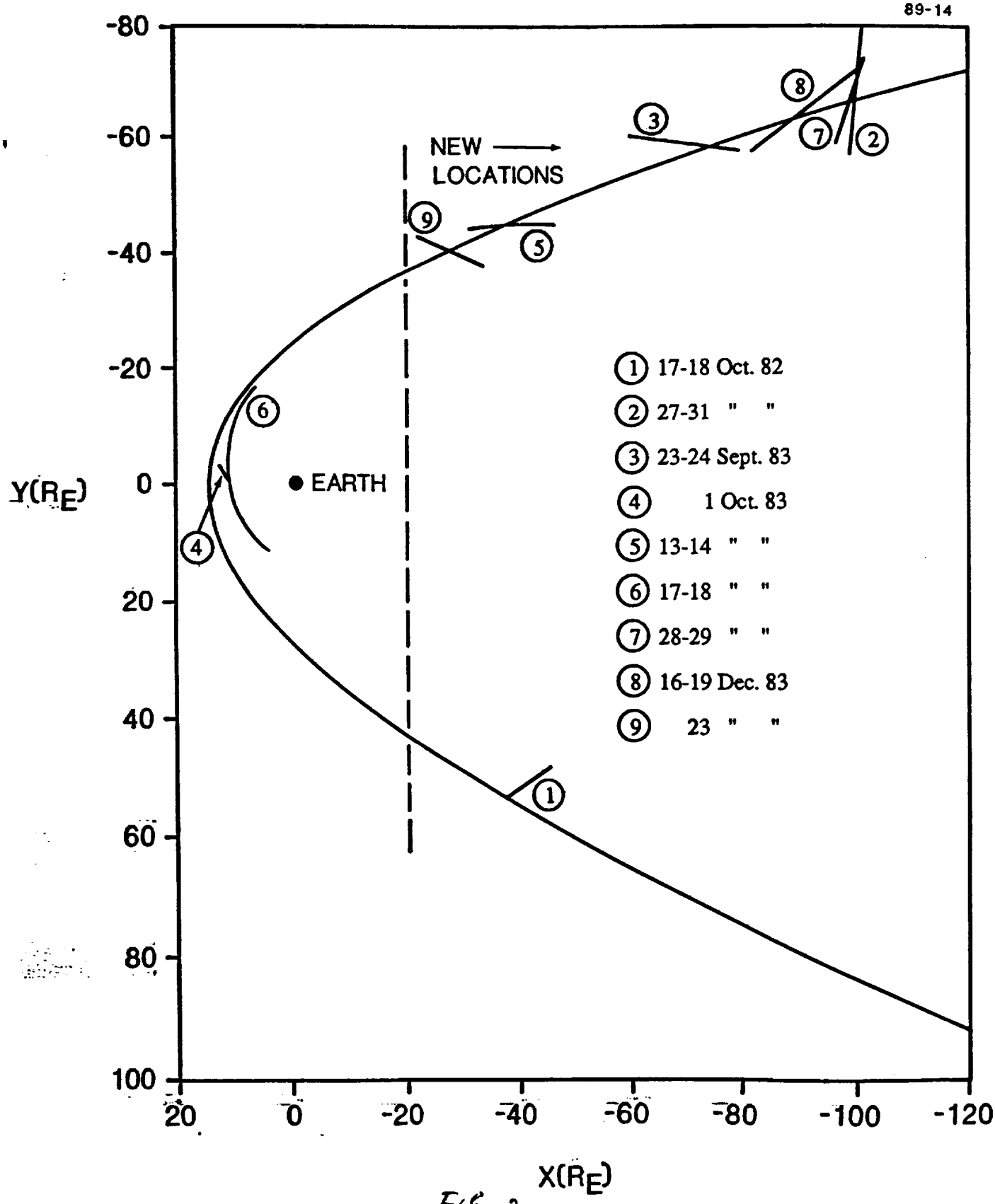

FIG. 2

SEGMENTS OF THE ISEE-3 TRAJECTORY THAT INCLUDED BOW SHOCK CROSSINGS WERE SPACED AT VARYING DISTANCES ALONG THE FLANK OF THE

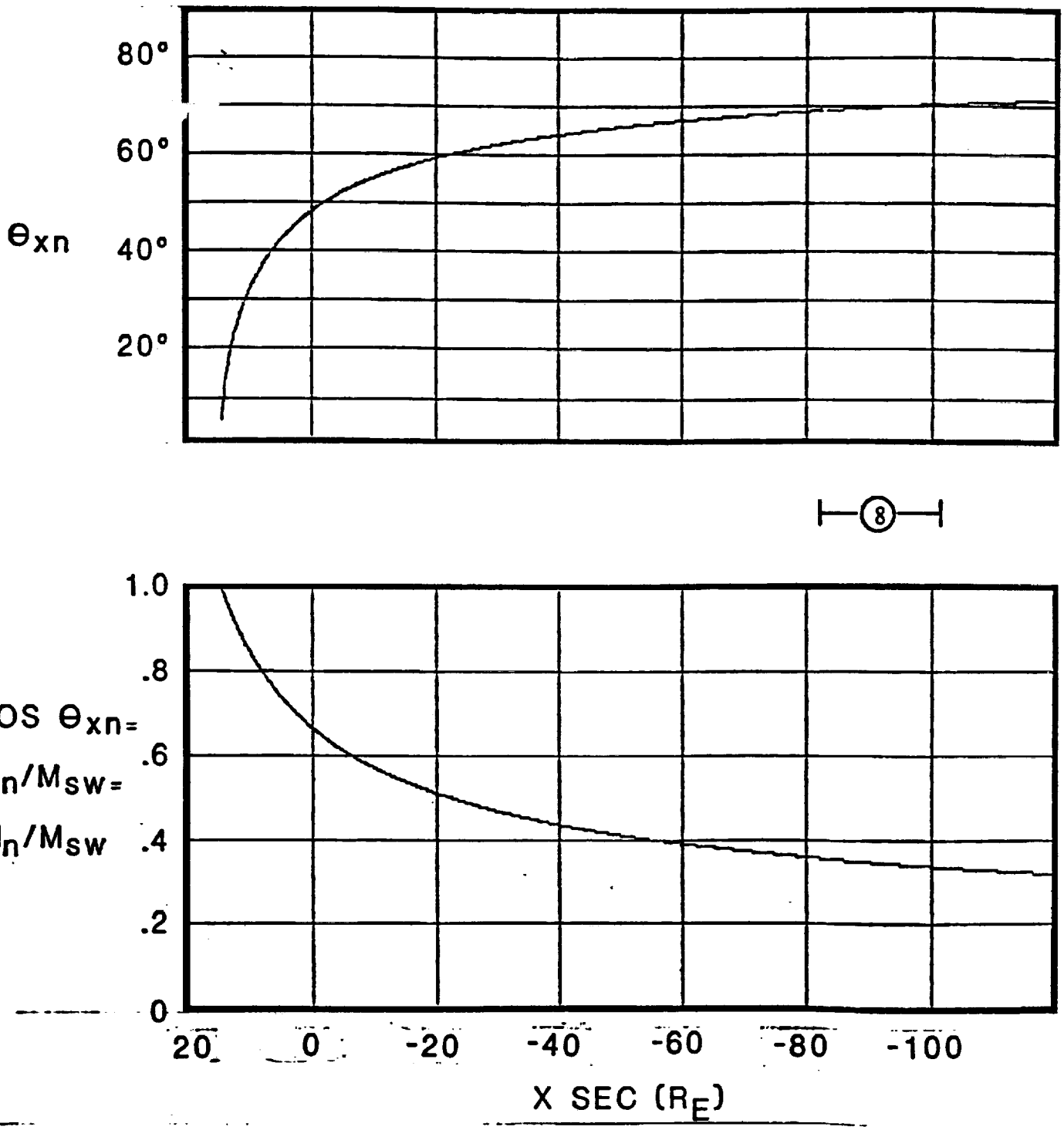

GOOD AGREEMENT OF THE DISTANT CROSSINGS WITH THE MODEL ENCOURAGES USE OF THE MODEL'S SLOPE TO CALCULATE THE ANGLE OF THE LOCAL NORMAL TO THE SOLAR WIND, θ_{XN}, AND THE FACTOR, $\cos\theta_{XN}$, BY WHICH THE FREE STREAM MACH NUMBER IS REDUCED TO ESTIMATE THE LOCAL MACH NUMBER OF EACH CROSSING.

FIG. 3

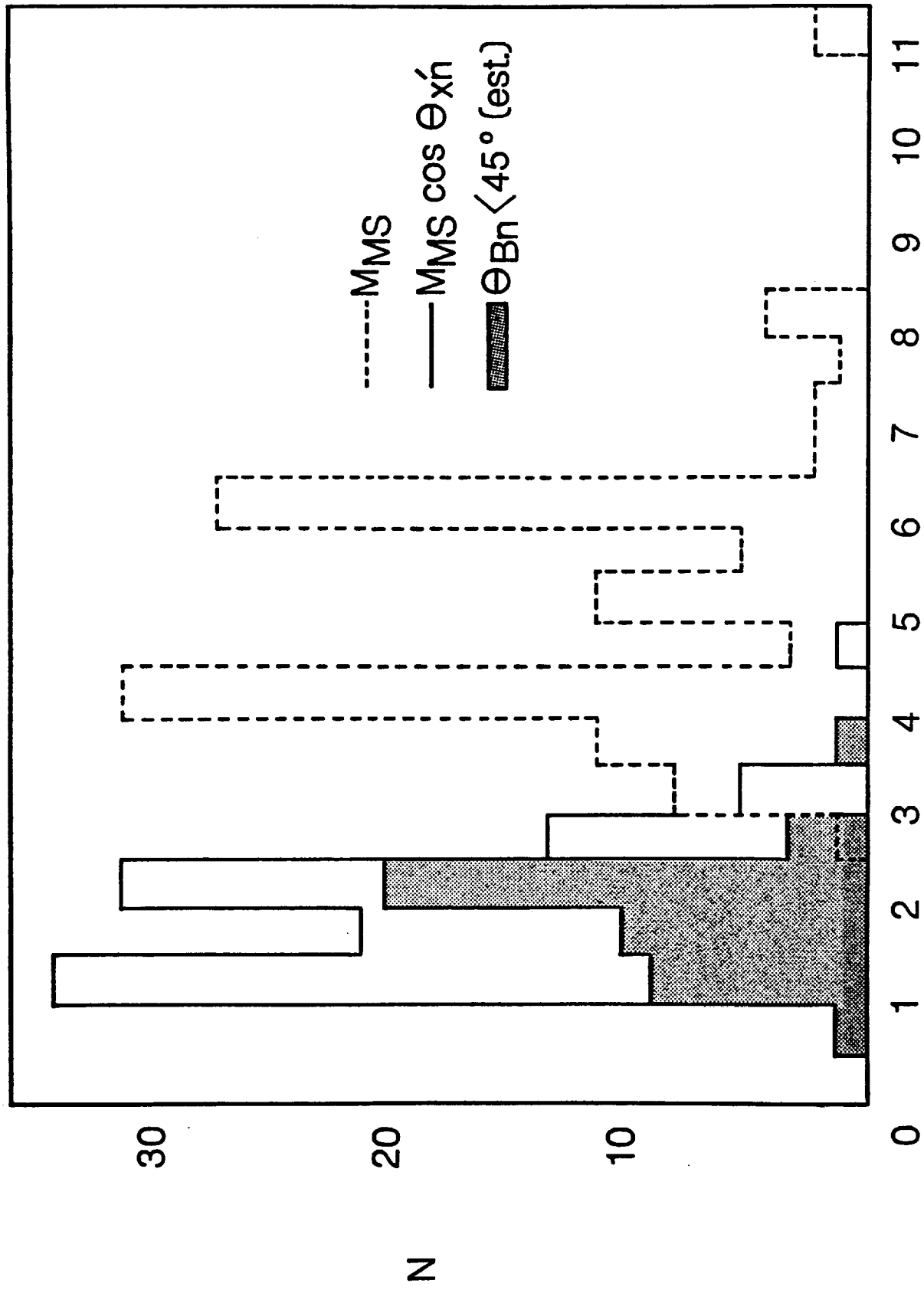
M_{MS}
M_{MS} cos $\Theta_{x'n}$
$\Theta_{Bn} < 45°$ (est.)
N
30
20
10
0
1
2
3
4
5
6
7
8
9
10
11
Mcos $\Theta_{x'n}$

Fig. 4

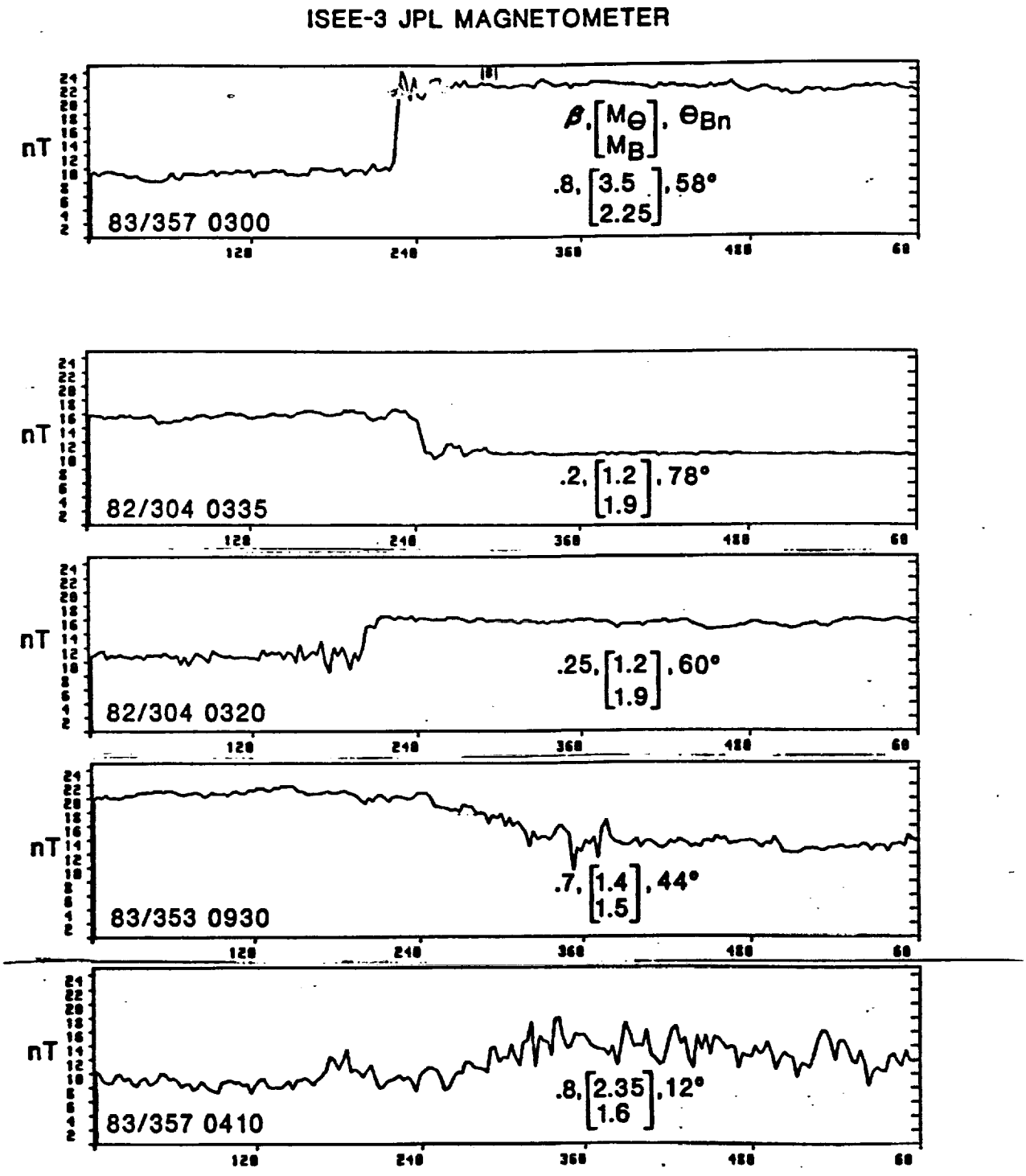
ISEE-3 JPL MAGNETOMETER
nT
83/357 0300
β, [MΘ / MB], ΘBn
.8, [3.5 / 2.25], 58°
82/304 0335
.2, [1.2 / 1.9], 78°
82/304 0320
.25, [1.2 / 1.9], 60°
83/353 0930
.7, [1.4 / 1.5], 44°
83/357 0410
.8, [2.35 / 1.6], 12°
Δt (sec)

FIG. 5

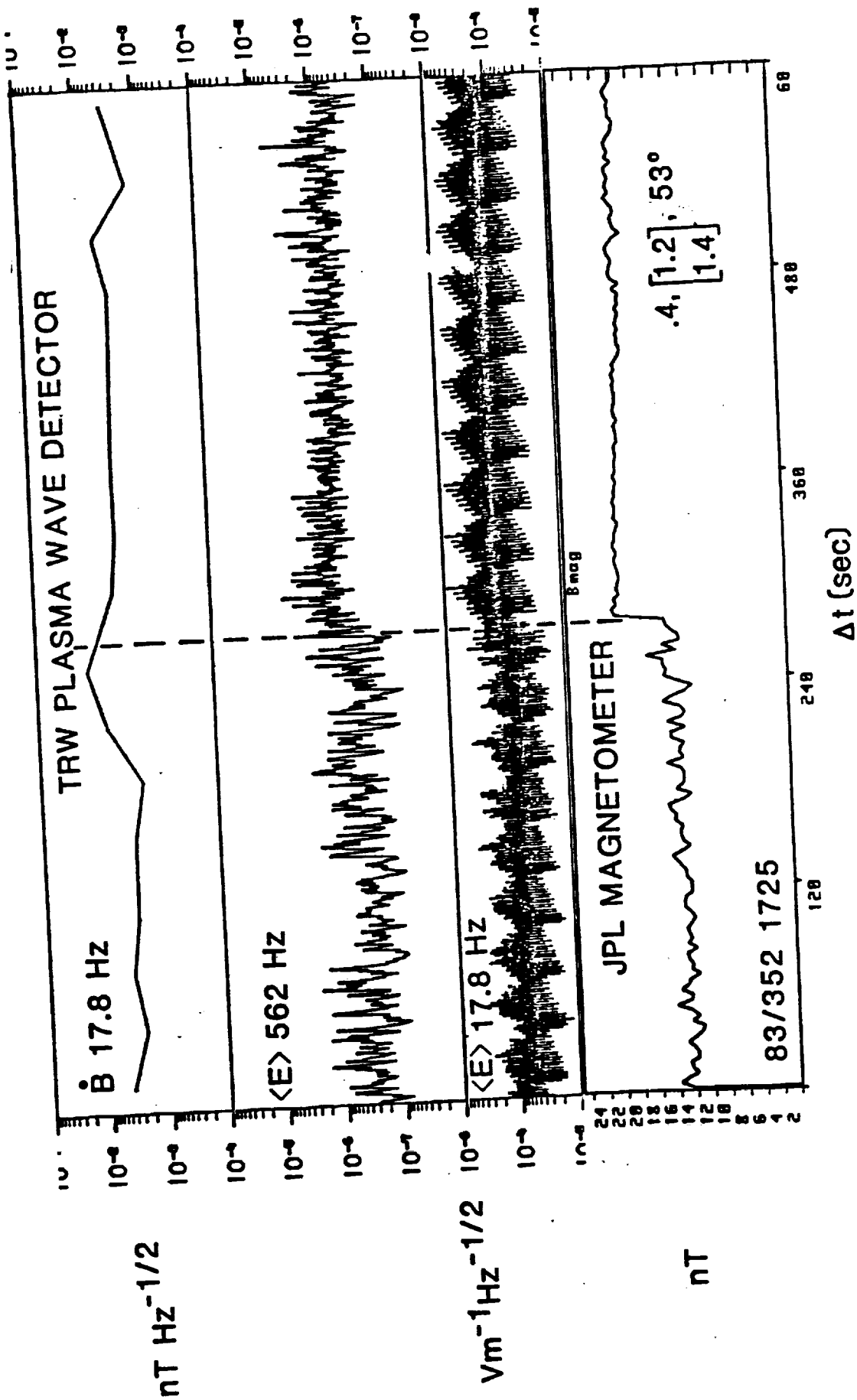
TRW PLASMA WAVE DETECTOR
B 17.8 Hz
<E> 562 Hz
<E> 17.8 Hz
JPL MAGNETOMETER
.4, [1.2] [1.4], 53°
83/352 1725
Δt (sec)
nT Hz^-1/2
Vm^-1Hz^-1/2
nT

Fig. 6

APPENDIX C

Abstract and first page of publication

Abstract and first page of publication

JOURNAL OF GEOPHYSICAL RESEARCH, VOL. 94, NO. A1, PAGES 49-59, JANUARY 1, 1989

Correlated Plasma Wave, Magnetic Field, and Energetic Ion Observations in the Ion Pickup Region of Comet Giacobini-Zinner

I. G. RICHARDSON,[1] K.-P. WENZEL,[2] S. W. H. COWLEY,[1] F. L. SCARF,[3,4] E. J. SMITH,[5] B. T. TSURUTANI,[5] T. R. SANDERSON,[2] AND R. J. HYNDS[1]

Relationships between simultaneous plasma wave, magnetic field, and energetic heavy ion data obtained by the International Cometary Explorer (ICE) spacecraft in the large-scale solar wind particle pickup region surrounding comet Giacobini-Zinner are examined. In particular, we investigate the conditions under which electrostatic emissions at frequencies of a few kilohertz and electromagnetic waves at a few tens of hertz are observed. It is shown that the data are consistent with the view that the kilohertz electrostatic emissions result from a beam-type instability excited by the pickup photoelectron population when the angle α between the magnetic field and the plasma velocity vectors is not too large ($\alpha < 60°$). The data also suggest that the few tens of hertz electromagnetic waves may be excited by a ring-type instability associated with the pickup ion population, which occurs when the magnetic field is near to orthogonality with the flow ($\alpha > 60°$).

1. INTRODUCTION

One of the most striking results to have emerged from the flyby of comet Giacobini-Zinner by the International Cometary Explorer (ICE) spacecraft in September 1985 [*von Rosenvinge et al.*, 1986] was the observation of a large-scale interaction region in the solar wind extending to radial distances of $\sim 4 \times 10^6$ km from the comet. In this region, heavy (predominantly water group) cometary ions with energies above a few tens of keV were observed streaming in the antisolar direction. Their intensities generally increased with decreasing distance to the comet, peaking near the boundary of the mass-loaded region of slowed flows at cometocentric distances of $\sim 10^5$ km [*Hynds et al.*, 1986; *Ipavich et al.*, 1986; *Sanderson et al.*, 1986*a*, *b*].

In the same region a number of distinctive plasma wave emissions were observed, which, like the ions, increased in intensity closer to the comet. Six main types of waves have been identified, covering more than 6 orders of magnitude in frequency. Starting at the lowest frequencies, waves of ~ 100-s period, corresponding to the water group ion gyroperiod in a typical interplanetary field of ~ 10 nT, were observed in the magnetometer data [*Tsurutani and Smith*, 1986*a*, *b*]. These waves produced significant angular deflections of the ambient magnetic field within distances of $\sim 10^6$ km of the comet, increasing in amplitude to give $\Delta B/B \simeq 1$ within the mass-loaded region. By considering the waveform, polarization, and associated plasma density fluctuations of these waves, *Tsurutani et al.* [1987] concluded that they belong to the magnetosonic (fast MHD) branch (i.e., right-hand polarized for parallel propagation), which costream with the cometary water group ions (toward the Sun in the solar wind rest frame) and are amplified by gyroresonant interactions with the ions. Within $\sim 3 \times 10^5$ km of the comet, packets of shorter-period (~ 1 s) waves were also observed on the steepened leading edges of the ~ 100-s waves [*Tsurutani and Smith*, 1986*b*; *Tsurutani et al.*, 1987], their frequency corresponding to about 10 times the proton cyclotron frequency, hence indicating waves of the whistler mode branch. At somewhat higher frequencies, search coil data showed the presence of waves with frequencies of several hertz, corresponding to the lower hybrid frequency (~ 6 Hz in a 10-nT field), together with emissions from a few tens to ~ 100 Hz [*Scarf et al.*, 1986, 1987; *Coroniti et al.*, 1986; *Kennel et al.*, 1986]. The latter emissions were also considered to be whistler mode waves by *Scarf et al.* [1986] on account of their electromagnetic nature and their frequency relative to the electron cyclotron frequency (~ 300 Hz in a ~ 10-nT field). Finally, electric field data showed the presence of waves in the frequency range from several hundred hertz to several kilohertz, termed "ion acoustic" waves by *Scarf et al.* [1986], together with bursts of waves near the electron plasma frequency (few tens of kilohertz). *Fuselier et al.* [1986] have shown that upstream from the comet bow shock ($\sim 10^5$ km) the waves near the electron plasma frequency occur in the presence of a sunward directed electron heat flux, indicating magnetic connection to the heated electron population in the region downstream from the shock [*Bame et al.*, 1986].

Since the large-scale region of enhanced wave activity coincides in broad terms with the region where streaming energetic ions were observed in the solar wind, it seems clear that these phenomena must be closely, if not directly, linked. The energetic ions are believed to originate from cometary neutrals, mainly water molecules, which sublime from the nucleus and expand outward, unrestrained by the comet's gravity, at typical speeds of ~ 1 km s^{-1}. These molecules are photodissociated to oxygen and hydrogen atoms on time scales of $\sim 10^5$ s and are then ionized either by solar UV photons or by charge exchange with solar wind ions on time scales of $\sim 10^6$ s, resulting in a region of cometary ion production (mainly protons and oxygen) in the solar wind extending several million kilometers from the comet.

Since the ions are created essentially at rest relative to the comet (and also relative to the spacecraft at the Giacobini-Zinner flyby, owing to the low ~ 21 km s^{-1} encounter speed), they subsequently move on cycloidal trajectories in the crossed electric and magnetic fields of the solar wind. During this motion the particle energy in the spacecraft frame varies

[1]Blackett Laboratory, Imperial College, London.
[2]Space Science Department, European Space Agency, European Space Research and Technology, Noordwijk, Netherlands.
[3]TRW Space and Technology Group, Redondo Beach, California.
[4]Deceased July 17, 1988.
[5]Jet Propulsion Laboratory, California Institute of Technology, Pasadena, California.

Paper number 88JA03597.
0148-0227/89/88JA-03597$05.00

APPENDIX D

Presentations and Publications, January 1985 to July 1988

APPENDIX D

Presentations and Publications, January 1985 to July 1988

The ISEE-C Plasma Wave Investigation (R.W. Fredricks, D.A. Gurnett, and E.J. Smith, 2nd, 3rd, and 4th authors), Geoscience Electronics, GE-16, 191, 1978.

Correlated Whistler and Electron Plasma Oscillation Bursts Detected on ISEE-3 (C.F. Kennel, F.V. Coroniti, R.W. Fredricks, D.A. Gurnett, and E.J. Smith, 1st, 3rd, 4th 5th, and 6th authors), Geophys. Res. Lett., 7, 129, 1980.

Energetic Electrons and Plasma Waves Associated with a Solar Type III Radio Burst (R.P. Lin, D.W. Potter, and D.A. Gurnett, 1st, 2nd, and 3rd authors), Astrophysical Journal, 251, 336, 1981.

Non-Local Plasma Turbulence Associated with Interplanetary Shocks (C.F. Kennel, F.V. Coroniti, E.J. Smith, and D.A. Gurnett, 1st, 3rd, 4th, and 5th authors), J. Geophys. Res., 87, 17, 1982.

Whistler Mode Turbulence in the Disturbed Solar Wind (F.V. Coroniti, C.F. Kennel, and E.J. Smith, 1st, 2nd, and 4th authors), J. Geophys. Res., 87, 6029, 1982.

Plasma Wave Levels and IMF Orientations Preceding Observations of Interplanetary Shocks by ISEE-3 (E.W. Greenstadt, C.F. Kennel, E.J. Smith, and R.W. Fredricks, 1st, 3rd, 4th, and 5th authors), Geophys. Res. Lett., 9, 668, 1982.

Science Return from ISEE-3 at Comet Giacobini-Zinner (E.J. Smith and R.W. Farquhar, 2nd and 3rd authors), Cometary Exploration II (Proceedings of International Conference on Cometary Exploration, Budapest, November 1982), 225, 1983.

The Interplanetary Shock Event of November 11/12, 1978 --A Comprehensive Test of Acceleration Theory (K.P. Wenzel, T.R. Sanderson, P. Van Nes, C.F. Kennel, F.V. Coroniti, C.T. Russell, G.K. Parks, E.J. Smith, and W.C. Feldman, 1st, 2nd, 3rd, 4th, 6th, 7th, 8th, 9th, and 10th authors), in Proceedings of the 18th International Cosmic Ray Conference, (Bangalore, India, August 1983), 131, 1983.

Plasma and Energetic Particle Structure Upstream of a Collisionless Quasi-Parallel Shock (C.F. Kennel, F.V. Coroniti, C.T. Russell, K.P. Wenzel, T.R. Sanderson, P. Van Nes, W.C. Feldman, G.K. Parks, E.J. Smith, B. Tsurutani, F.S. Mozer, M. Temerin, R.R. Anderson, J. Scudder, and M. Scholer, 1st, and 3rd through 16th authors), J. Geophys. Res., 89, 5419, 1984.

Structure of the November 12, 1978, Quasi-Parallel Interplanetary Shock (C.F. Kennel, J.P. Edmiston, F.V. Coroniti, C.T. Russell, E.J. Smith, B. Tsurutani, J. Scudder, W.C. Feldman, R.R. Anderson, F.S. Mozer, and M. Temerin, 1st, 2nd, and 4th through 12th authors), J. Geophys. Res., 89, 5436, 1984.

Plasma Waves in Space, Radiation in Plasma, ed. B. McNamara, (World Scientific Publishing Co., Singapore), p. 103, 1984.

ISEE-3 Wave Measurements in the Distant Geomagnetic Tail and Boundary Layer (F.V. Coroniti, C.F. Kennel, R.W. Fredricks, D.A. Gurnett, E.J. Smith, 2nd through 6th authors), Geophys. Res. Lett., 11, 335-338, 1984.

Continuum Radiation and Electron Plasma Oscillation in the Distant Geomagnetic Tail (F.V. Coroniti, C.F. Kennel, and D.A. Gurnett, 1st, 3rd, and 4th authors), Geophys. Res. Lett., 11, 661, 1984.

Substorm Associated Traveling Compression Regions in the Distant Tail: ISEE-3 Geotail Observations (J.A. Slavin, E.J. Smith, B.T. Tsurutani, D.G. Sibeck, G.L. Siscoe, H.J. Singer, D.N. Baker, J.T. Gosling, and E.W. Hones, 1st through 9th authors), Geophys. Res. Lett., 11, 657, 1984.

Magnetotail Flux Ropes (D.G. Sibeck, G.L. Siscoe, J.S. Slavin, E.J. Smith, and J.G. Gosling, 1st through 5th authors), Geophys. Res. Lett., 11, 1090, 1984.

Plasma Wave Spectra Near Slow Mode Shocks in the Distant Magnetotail (F.V. Coroniti, C.F. Kennel, E.J. Smith, J.A. Slavin, B.T. Tsurutani, S.J. Bame, and W.C. Feldman, 2nd through 7th authors), Geophys. Res. Lett., 11, 1050, 1984.

ISEE-3 Plasma Wave Observations in the Earth's Geomagnetic Tail, published in the Proceedings of the Japan/U.S. Workshop on Science Objectives of the Geotail Mission, March 13-14, 1985, Institute of Space and Astronautical Science, Tokyo, Japan, p. 27, 1985.

The 1985-86 Spacecraft Missions to Comets Giacobini-Zinner and Halley, Advances in Space Plasma Physics, ed. B. Buti, World Scientific Publishing Company, p. 22, 1985.

ELF - Emissions from Interplanetary Shocks Observed on Prognoz-8 and ISEE-3 (O. Vaisberg, N. Borodkova, and M. Nozdratchev, 1st, 3rd, and 4th authors), published in the Proceedings of the Solar Maximum Analysis Symposium, Irkutsk, USSR, June 17-21, 1985.

Evidence for Nonlinear Wave-Wave Interactions in Solar Type III Radio Bursts (R.P Lin, W. Lotko, and D.A. Gurnett, 1st, 2nd, and 3rd authors), Astrophysical Journal, 308, 994, 1986.

Coordinated Multispacecraft Plasma Science in the Solar Wind and Comet Plasma Environments (IACG WG-2) (A.A. Galeev, 1st author), ESA SP-1066, "Space Missions to Halley's Comet and the Inter-Agency Consultative Group," p. 233, 1986.

A Test of Lee's Quasi-Linear Theory of Ion Acceleration by Interplanetary Traveling Shocks (C.F. Kennel, F.V. Coroniti, W.A. Livesey, C.T. Russell, E.J. Smith, K.P. Wenzel, and M. Scholer, 1st, 2nd, 4th, 5th, 6th, 7th, and 8th authors), J. Geophys. Res., 91, 11,917-11,928, 1986.

Plasma Waves in Magnetotail Flux Ropes (C.F. Kennel and F.V. Coroniti, 1st and 2nd authors), J. Geophys. Res., 91, 1414, 1986.

Plasma Wave Observations at Comet Giacobini-Zinner (F.V. Coroniti, C.F. Kennel, D.A. Gurnett, W-H. Ip, and E.J. Smith, 2nd, 3rd, 4th, 5th, and 6th authors), Science, 232, 377, 1986.

Prospects for Plasma Wave Correlations: 1984-86, published in "Proceedings International Workshop on Field Particle and Wave Experiments on Cometary Missions," Graz, pp. 211-213, 1986.

Heat Flux Observations and the Location of the Transition Region Boundary of G-Z (S.A. Fuselier, W.C. Feldman, S.J. Bame, and E.J. Smith, 1st, 2nd, 3rd, and 4th authors), Geophys. Res. Lett., 13, 247, 1986.

Dust Particles Detected Near Giacobini-Zinner by the ICE Plasma Wave Instrument (D.A. Gurnett, T.F. Averkamp, and E. Grun, 1st, 2nd, and 4th authors), Geophys. Res. Lett., 13, 291, 1986.

Plasma Wave Turbulence in the Strong Coupling Region at Comet Giacobini-Zinner (F.V. Coroniti, C.F. Kennel, E.J. Smith, B.T. Tsurutani, S.J. Bame, M.F. Thomsen, R. Hynds, and K.P. Wenzel, 1st, 2nd, 4th through 9th authors), Geophys. Res. Lett., 13, 869, 1986.

Plasma Waves in the Shock Interaction Regions of Comet Giacobini-Zinner (C.F. Kennel, F.V. Coroniti, B.T. Tsurutani, E.J. Smith, Jr., S.J. Bame, and J.T. Gosling, 1st, 2nd, 4th, 5th, 6th, and 7th authors), Geophys. Res. Lett., 13, 921, 1986.

A Storm Time, Pc 5 Event Observed in the Outer Magnetosphere by ISEE 1 and 2: Wave Properties (E.W. Greenstadt, R.L. McPherron, R.R. Anderson, 1st-3rd authors), J. Geophys. Res., 91, 13,398-13,410, 1986.

ICE Plasma Wave Measurements in the Ion Pick-Up Region of Comet Halley (F.V. Coroniti, C.F. Kennel, T.R. Sanderson, K.P. Wenzel, R.J. Hynds, E.J. Smith, S.J. Bame, and R.D. Zwickl, 2nd through 9th authors), Geophys. Res. Lett., 13, 857, 1986.

Characteristics of the Tail of Comet Giacobini-Zinner, Advances in Space Research, 6, 329, 1986.

Plasma Wave Observations for Comet Flyby Missions, to be published in the Proceedings of the Symposium on the Multi-Comet Sample Return Mission, 1986.

The P/Giacobini-Zinner Magnetotail (J.A. Slavin, E.J. Smith, P.W. Daly, K.R. Flammer, G. Gloeckler, B.A. Goldberg, D.J. McComas, and J.L. Steinberg (1st, 2nd, 3rd, 4th, 5th, 6th, 7th, and 9th authors), Proceedings of the 20th ESLAB Symposium on the Exploration of Halley's Comet, Heidelberg, Vol. 1, p. 81, 1986.

MHD Waves Detected by ICE at Distances > 28 x 10^6 km from Comet Halley: Cometary or Solar Wind Origin? (B.T. Tsurutani, A.L. Brinca, E.J. Smith, R.M. Thorne, J.T. Gosling, and F.M. Ipavich, 1st, 2nd, 3rd, 4th, 6th, and 7th authors), Proceddings of the 20th ESLAB Symposium on the Exploration of Halley's Comet, Heidelberg, Vol. III, p. 451, 1986.

Analysis of the Giacobini-Zinner Bow Wave (E.J. Smith, J.A. Slavin, S.J. Bame, M.F. Thomsen, S.W.H. Cowley, I.G. Richardson, D. Hovestadt, F.M. Ipavich, K.W. Oglivie, M.A. Coplan, T.R. Sanderson, K.P. Wenzel, A.F. Vinas, and J.D. Scudder, 1st through 12th, 14th, and 15th authors), Proceedings of the 20th ESLAB Symposium on the Exploration of Halley's Comet, Heidelberg, Vol. III, p. 461, 1986.

Observations of Cometary Plasma Wave Phenomena (F.V. Coroniti, C.F. Kennel, D.A. Gurnett, W.H. Ip, and E.J. Smith, 2nd through 6th authors), Proceedings of the 20th ESLAB Symposium on the Exploration of Halley's Comet, Vol. I, p. 163, 1986; Astronomy and Astrophysics, 187, 109, 1987.

A Comparison Between Wave Observations Performed in the Environments of Comets Halley and Giacobini-Zinner (R. Grard, J.G. Trotignon, and M. Mogilevsky, 1st, 3rd, and 4th authors), in press, Proceedings of the Symposium on the Diversity of Comets, Brussels, 6-9 April 1987, and Similarity ESA SP-278, 97, September 1987.

Plasma Physics Phenomena Detected at Comet Giacobini-Zinner, to be published in Cometary and Solar Plasma Physics (World Scientific Publishing Co.), edited by B. Buti, 1987.

Plasma Waves Near Collisionless Shocks (S.L. Moses, C.F. Kennel, E.W. Greenstadt, and F.V. Coroniti, 2nd, 3rd, 4th, and 5th authors), Proceedings of the International Symposium on Collisionless Shocks, Balaton, Hungary, 1987, p. 19.

Plasma Wave Observations at Comets Giacobini-Zinner and Halley, in the Proceedings of the Sendai Chapman Conference on Plasma Waves and Instabilities in Magnetospheres and at Comets, H. Oya and B.T. Tsurutani, eds., Tokoku Univ., Sendai, Japan, 36-39, 1988.

The Search for Lower Hybrid Drift Turbulence in Slow Shocks (F.V. Coroniti, C.F. Kennel, B.T. Tsurutani, and E.J. Smith, 1st, 3rd, 4th, and 5th authors), J. Geophys. Res., 93, 2553-2561, 1988.

Local Generation of Electrostatic Bursts at Comet Giacobini-Zinner: Modulation by Steepened Magnetosonic Waves (Armando L. Brinca and B.T. Tsurutani, 1st and 2nd authors), J. Geophys. Res., 94, 60-64, 1989.

Correlated Plasma Wave, Magnetic Field and Energetic Ion Observations in the Ion Pickup Region of Comet Giacobini-Zinner (I.G. Richardson, K.P. Wenzel, S.W.H. Cowley, E.J. Smith, B.T. Tsurutani, T.R. Sanderson, and R.J. Hynds, 1st, 2nd, 3rd, 5th, 6th, 7th, and 8th authors), J. Geophys. Res., 94, 49-59, 1989.